Wacker *et al. ROBOMECH Journal* (2024) 11:1
https://doi.org/10.1186/s40648-023-00270-y

ROBOMECH Journal

RESEARCH ARTICLE

Open Access

Experimental assessment and prediction of design parameter influences on a specific vacuum-based granular gripper

Christian Wacker[1*], Niklas Dierks[2], Arno Kwade[2] and Klaus Dröder[1]

Abstract

Innovative soft robotic grippers, such as granular grippers, enable the automated handling of a wide spectrum of different geometries, increasing the flexibility and robustness of industrial production systems. Granular grippers vary in their design as well as in their configuration, which affects the specific characteristics and capabilities regarding grippable objects. Relevant aspects are the selection of granulates and membranes, as they affect the deformability. This influences the achievable gripping forces, which vary with the gripped objects geometry. On the basis of experimental studies, the modeling of interpolations as well as through experimental validations, the present research investigates the influences of different configurations on the achievable gripping forces for a specific concept of an innovative vacuum-based granular gripper. Specifically, the focus lies on design as well as configuration parameters, which could influence the achievable gripping force. Influencing parameters are determined based on a literature review of similar gripping concepts. Various adjustment possibilities are identified, such as materials of granulates or membranes. The possible configuration options are experimentally analyzed with a one-factor-at-a-time approach. The possibility of modelling the effects of their interrelations on the achievable gripping force is examined with approaches for linear models and compared to interpolations based on Machine Learning. Especially the granulate filling level and the membrane configuration exhibit the largest influences, which were best predicted with the approach based on artificial neural networks. A selection of an optimized gripper configuration for a specified object set as well as possible further developments such as a continuous expandability of the approaches and integrations with simulations are discussed. As a result of these analyses, this research provides methodologies for an optimized selection of a gripper configuration for an improved object-specific achievable gripping force and allows for more efficient handling processes with the examined type of vacuum-based granular gripper.

Keywords Modeling, Prediction, Gripping, Handling, End effectors

Introduction

Handling is one of the most widespread and basic tasks necessary for an automated and efficient production of goods. In order to achieve the handling of objects as effectively as possible, the end effectors and grippers used for these systems have to be capable of securely handling the gripped objects without detachment during the handling process. Typically, this is done by utilizing predefined points on the object's geometry, where the selected grippers characteristics, such as a mechanical or a vacuum-based suction cup gripper are easy to predict

*Correspondence:
Christian Wacker
c.wacker@tu-braunschweig.de
[1] Institute of Machine Tools and Production Technology, Technische Universität Braunschweig, 38106 Brunswick, Germany
[2] Institute for Particle Technology, Technische Universität Braunschweig, 38104 Brunswick, Germany

and enable high gripping forces [1]. Within these conditions, the gripping strength or vacuum can be adjusted in accordance to the object's weight and the specific handling task [2]. With these widespread conventional grippers, usually flat and uniform surfaces are required, which have to be detected precisely in order to guarantee a secure and faultless grip [3].

Additional process-specific factors can complicate some handling tasks, such as the handling of unpredictably shaped objects. This would be the case for products of nature or worn-out components at the end of their individual life cycles. Precise positioning of grippers on specifically defined surface areas in scenarios for picking from a moving conveyor belt or from a bin with randomly placed loose items is also often challenging. These types of handling procedures are complex, as an exact analysis of the position and surface characteristics of the gripped object and its interrelations with a successful gripping would require significant implementation of cameras, sensors or other hardware and is therefore often prohibitively expensive [4, 5].

To address these challenges, new gripping solutions, such as granular grippers, designed for a versatile handling with a wider capability and tolerance towards more complex surfaces are developed [6, 7]. These innovative grippers could improve the efficiency and effectiveness of automated handling tasks in multiple ways:

- A single gripper could be capable of gripping different surfaces without necessitating a swapping out of the gripper [2, 8]
  - Reduced complexity of the handling setup for gripping various object shapes within a singular handling use case
  - Increased flexibility for swapping between handling stations with entirely different handling tasks
- A gripper could offer a wider versatility and tolerance to somewhat unpredictable environmental conditions [8]
  - Reduced necessary tolerance for measuring or placement systems e.g. during bin picking
  - More tolerance for individual components with a wide tolerance of characteristics, such as natural raw materials with varying and undefined surface structures

Within the following research, experimental investigations as well as modeling approaches regarding achievable gripping forces of such an innovative gripper are explored.

Examined vacuum-based granular gripper

A possible solution for versatile handling are granular grippers. Usually, these grippers consist of an airtight membrane or'cushion' filled with granulate material. In an unactuated state, this gripper is deformable and capable of adapting to a wide range of geometries. When the system is actuated and a vacuum is applied to the gripper, both the membrane and the granulate filling contracts, referred to as a 'jammed' state (see Fig. 1a). According to Goetz et al., Fitzgerald et al. and Brown et al. [9–11], three different effects enable a gripping force, which can be differentiated as the following:

1. Geometric interlocking of the object and the 'jammed' gripper
2. Static friction between the object and the membrane
3. Suction effects, where the membrane and the surface of the object create an air-tight seal

Usually, the suction effects as well as the geometry interlocking are by far the most significant influences [11]. These suction effects are largely dependent on the membrane, where a contraction of membrane and granulate results in a small volume of reduced pressure. The sealing and low pressure area creating the suction effect is shown in Fig. 1b) as a section from an X-ray tomogram [12].

When handled objects are larger than the gripper itself, the influence of geometric interlocking is often negligible, especially for surfaces with fewer three-dimensional protruding geometries. As a result, conventional granular grippers are generally unsuitable or unfeasible for widespread applications such as handling mostly flat metal sheets. They are mainly used for either objects smaller than the gripper or objects with distinct protruding geometries, where a secure grip can be achieved.

In an attempt to combine the possibilities of the form-fitting properties of granular grippers with the ability to securely grip objects with less prominent features, a modification of the conventional granular gripper was developed at TU Braunschweig [13–15]. In this approach, the mechanism of achieving successful gripping through suction effects is replaced (Fig. 2a)) and improved upon by actively supporting the suction with a permeable membrane at the gripper-object-interface (GOI) (Fig. 2b)).

When the pressure difference is applied by an external vacuum pump, the gripper retains the 'jamming' properties; however, the gripping force is supported by the additional vacuum gripping effects facilitated by the porous area at the GOI. Depending on the geometry of the gripped object, these additional vacuum gripping effects can account for large parts of the resulting gripping force [16].

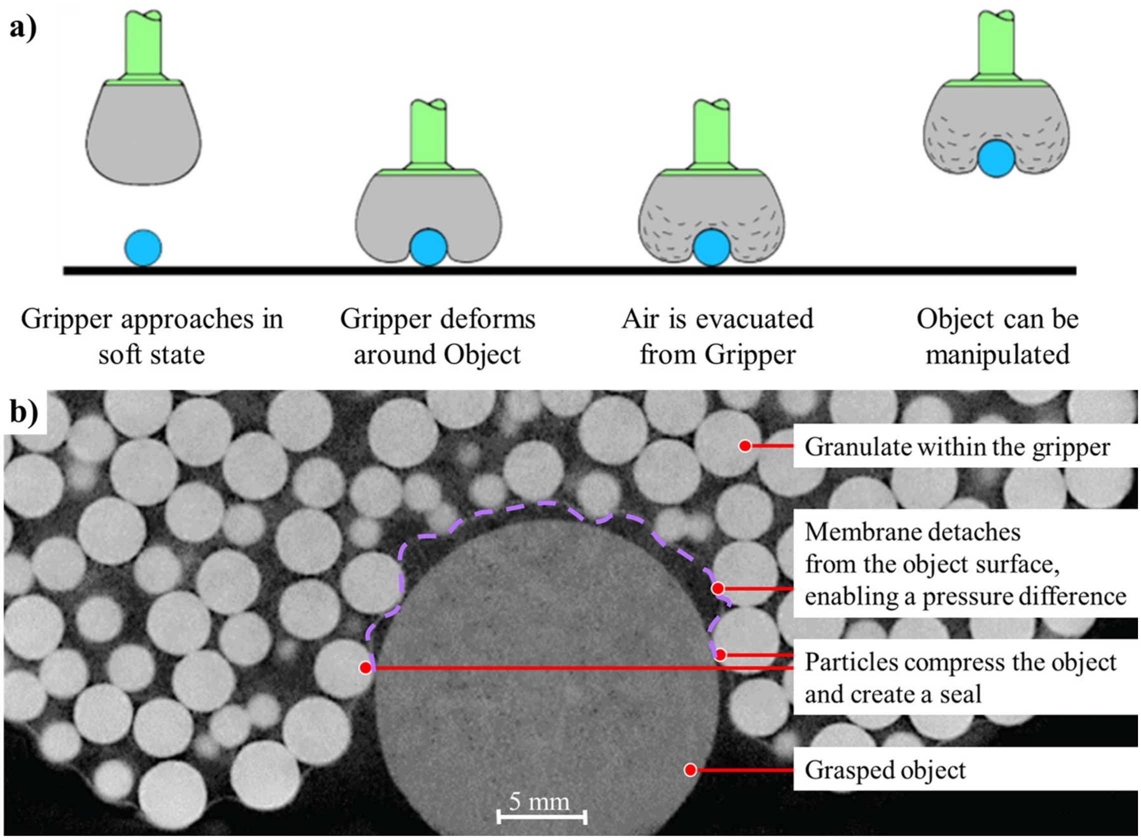

Fig. 1 **a** Schematic for the gripping process with granular grippers [11]; **b** X-ray tomogram slice after evacuation around a round object with detached membrane marked in purple [12]

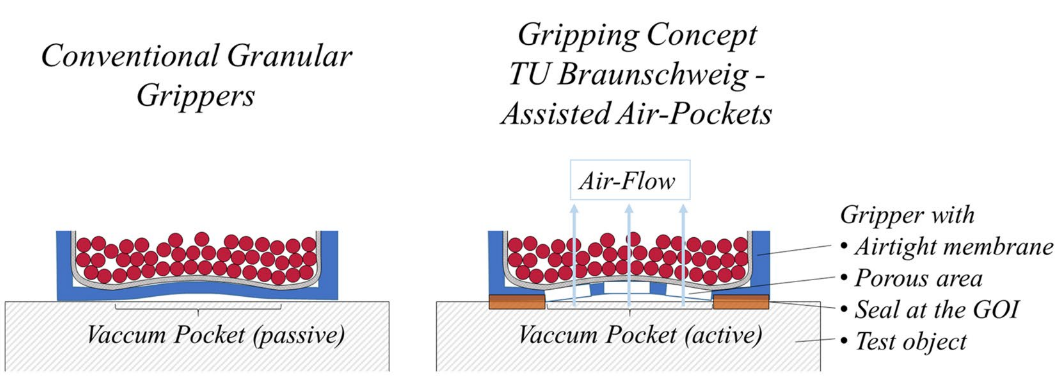

Fig. 2 Schematics of conventional granular grippers and the expanded concept examined within this study

Even though these grippers are often referred to as 'universal', their effectivity varies with its configuration and the gripped geometries. A granular handling-based gripper system can be configured in various different ways. Its gripping capabilities are influenced by a variety of characteristics and features, which mainly depend on the used granulate material, the membrane and possible design modifications. An example could be the filling ratio of these grippers, which could have different effects on the gripping forces for convex or concave objects. In order to utilize such a gripper in an industrial setting, its characteristics have to be assessable especially in regards to their achievable gripping force, and, if possible, optimized to an individual application with its specific process conditions. Enabling this optimization as well as a possible general estimation of the different design influences is the main objective of the present study. The results of various settings of influencing parameters are generally assessed by their effects on the grippers handling performance, therefore the following chapters examine the achievable gripping forces for different objects [2, 10, 16–21].

Goals for the examination of the influencing parameters and further structure

Within this context, the key questions regarding the configuration of this gripper for an increased understanding of the behavior and its optimization are:

- What is the influence of the various configuration characteristics on the achievable gripping force for the specific examined gripper design?
- Are these influences interrelated and how can configuration-specific gripping characteristics for different object geometries be predicted without extensive experiments?
- How can a prediction of achievable gripping forces for a specific spectrum of object geometries be implemented, considering the potential design variants and a prediction of a reliable handling regarding the standard deviation?

Additionally, soft robotic grippers in general are in a state of continuous development and adaptions to specific use cases are common. Therefore, a transferability of results between adapted gripper designs should be analyzed in some manner. Consequently, an additional research question should be investigated:

- Is it feasible to integrate knowledge and characteristics of different gripper designs for further adapted grippers?

As a key goal of the present research, a comprehensive investigation of the influences of different parameters on the examined gripper concept should be provided. For this, all relevant factors for the gripper configuration have to be identified and experimentally investigated regarding their influence on the achievable gripping force. If possible, a methodology should be derived from these analyses in order to find an ideal gripper configuration for individually composed object requirements. To enable this, the following chapters strive to do the following:

- Analyze current research for influences of design and configuration for granular grippers. (Chapter 1.3)
- Draw conclusions to possible influences for the specific examined gripper. (Chapter 1.4)
- Align these conclusions with previous research for the examined specific gripper. (Chapter 2)
- Design experiments for an initial examination of the defined influences. (Chapter 2.1)
- Examine the interaction and relevance of the identified influences experimentally. (Chapter 3)
- Discuss statistical prerequisites for predicting and modeling configuration influences and resulting gripping forces. (Chapter 4)
- Discuss an overall procedure for the selection of suitable configurations with a comparison of necessary predictions of the influences through linear models as well as Machine Learning. (Chapter 5)
- Validate the models by evaluating the predictions for selected experiments. (Chapter 6)
- Discuss possible future improvements and expansions. (Chapter 7)
- Conclude key results of the investigations of this research. (Chapter 8)

Previous research regarding influencing parameters for granular grippers

In the following chapter, an overview regarding current research for the various influences of configuration parameters on granular grippers is given. These publications mostly focus on the commonly used concept of the conventional granular gripper (see Fig. 2a)), especially the main two components granulate and membrane. The different examined influences of materials on the resulting gripping forces are summarized with some examples for publications in Tables 1 and 2 and discussed regarding their key results.

Previous research regarding the variation of granulates

Granulate material size is often described as one of the most influential parameters [30], as it affects the jamming behavior by changing the number of contact and slip points. Some researchers even describe it as the most critical property for the jamming performance [23] with varying results, such as Gomez-Paccapelo et al. describing a negative influence of granulate material larger than 1/15 of the target object diameter [29]. Researchers such as Athanassiadis et al. [31] and Howard et al. [28] further explored this improved jamming by examining the influences of particular shapes and recommend polyhedral shapes for the largest range in stiffness.

The variation of the granulate size is often combined with the material type, such as for sawdust and coffee [25], where the inherent material properties were described as 'small and big'. The fill level or filling ratio is often presented as another important factor [10], with researchers such as Fujita et al. [26]

Table 1 Overview of various publications for the granulate influences on gripping forces for granular grippers with information regarding the used granulate as well as the experimental approach with the number of repetitions for each object (trial size) as well as number of investigated grasped object geometries (shape count)

Publication			Variation of Granulates				Experimental Approach/ Results			
Refs.	Author	Year	Size	Material type	Filling ratio	Other	Trial Size	Shape count	Std Dev	Max Force
[22]	Amend et al.	2012	–	–	–	–	10	7	> 50% possible	Up to 20 N
[17]	Nishida et al.	2014	–	Adzuki beans, Aromatic beads and Ground coffee	20 to 80%	–	–	1	> 50% possible	Up to 30 N
[23]	Amend et al.	2016	12–20 mesh up to 60–100 mesh	–	–	–	–	7	–	Up to 90 N
[24]	Meuleman et al.	2017	2.5/ 4 mm	–	–	Matte/ Pol. glass	9	1	> 50% possible	Up to 10 N
[25]	Alsakarneh et al.	2018	'Small and Big'	Sawdust/ Coffee	–	Water Contents	3	1	up to 10%	< 1 N
[26]	Fujita et al.	2018	–	–	20 to 100%	–	10	1	> 50% possible	–
[27]	Miettinen et al.	2019	0.5—6 mm	Wood, Plastic, Sand, Rubber	–	–	Multiple	6	–	> 1000 N
[28]	Howard et al.	2021	3 sizes (3/ 5/ 7 mm) of 4 Grain Shapes	–	–	Grain shape	5	4	> 50% possible	Up to 15 N
[9]	Goetz et al.	2021	4/ 4.2 mm	Glas and Polystyrene	–	–	6	1	< 20%	Up to 20 N
[12]	Santarossa et al.	2022	120 µm/ 4 mm	–	–	–	6	1	> 50% possible	Up to 5 N
[29]	Gomez–Paccapelo et al.	2022	120 µ—2.5 mm	Polymer, Sand, Ceramic, Amaranth, Glass Small/ Large	–	–	5 to 10	1	< 5%	Up to 20 N

Table 2 Overview of various publications for the membrane influences on gripping forces for granular grippers with information regarding the varied membrane as well as the experimental approach with the number of repetitions for each object (trial size) as well as number of investigated grasped object geometries (shape count)

Publication			Variation of membranes		Experimental approach/ Results			
Refs.	Author	Year	Shape	Material type	Trial size	Shape count	Std Dev	Max force
[34]	Jiang et al.	2014	–	Vitrile, Vinyl, Nitrile, Latex and Polythene	3	–	–	–
[23]	Amend et al.	2016	Various	Rubbers, Silicones and Polyurethanes	–	7	–	Up to 90 N
[35]	Howard et al.	2022	Various	–	5	4	–	Up to 30 N

recommending 50% of the possible volume for an ideal gripping force. In some cases, further granulate parameters were examined, such as the water contents in sawdust [25] or the influences of granulate surface roughness [24] on the possible gripping forces. Most researchers utilized easily available or purchasable granulate materials and sizes with some examples of additive manufacturing [28]. Putzu et al. [32] and Goetz et al. [9] particularly focus on the possible positive influences of soft particles, describing it as a 'squeezing effect between the object and the gripper', which enables the GOI to have a larger contact area. Additionally, the influence of granulate materials on the necessary initial contact force for the molding to different geometries was examined [15, 33]. Size, material type, filling ratio as well as less frequently investigated parameters such as shape, roughness or elasticity are therefore identified as possible influences of granulate material. Previous studies suggested no major interrelations between the influencing parameters of the gripper configuration [25]. This should also be analyzed for the examined gripper.

Previous research regarding the variation of membranes

In comparison, membrane materials were varied less often (see Table 2), with elastomers, rubbers, nitriles and silicones being the most commonly used [23, 34]. Howard et al. [35, 36] and Amend et al. [23] also varied the shape of the grippers, with Howard et al. [35] implementing algorithms for an improvement of 3D-printed membrane shapes.

Research regarding different membranes for the gripping concept developed at TU Braunschweig previously focused on the air-permeability of the porous area at the GOI [14], recommending materials with a nominal air conductivity of over 200 1/(s·Pa) for this task. Concluding, especially the membrane materials as well as gripper-specific parameters such as design or air-permeability are relevant as possible influences for further investigations.

Trial sizes and standard deviations

Most previous researchers were either unspecific about the number of conducted experiments or used sample sizes (trial size) below ten repetitions per object. The number of different grasped geometries (shape count) was also usually below ten. In general, the standard deviation (Std. Dev.) for granular grippers is a large percentage, often over 50% of the gripping force, as the placement of the granulate material is unpredictable and tends to be slightly different for subsequent handling cycles. The gripping force itself depends on the size of the gripper, with researchers primarily focusing on small grippers on a laboratory scale and few examples for large-scale applications [27]. In order to enable an increased comprehensibility and transferability of the created knowledge, sample sizes with more than ten repetitions for object sets comprising at least ten different objects should be examined. Especially the resulting standard deviation is relevant for possible further industrial implementations in order to enable an assessment of the statistical confidence of a secure handling.

Specific gripping solution examined within this research and relevance of influencing parameters

The specific gripper developed at TU Braunschweig differs from conventional granular grippers through its characteristic added air permeability and resulting air flow (see Figs. 2, 3 and 4). This differentiation is relevant for both the granulate and the membrane parameters, as a continuous air-flow through the granulate as well as the porous area in the membrane are necessary for the operation of the gripper.

Relevance of granulate variations for the specific examined gripper

The potential influences of granulate material identified within the previous chapters include size, material, roughness, elasticity, filling ratio as well as shape. Additionally, due to the continuous air-flow through the gripper in the expanded concept, air-permeable hollow granulate material could also have an effect on the

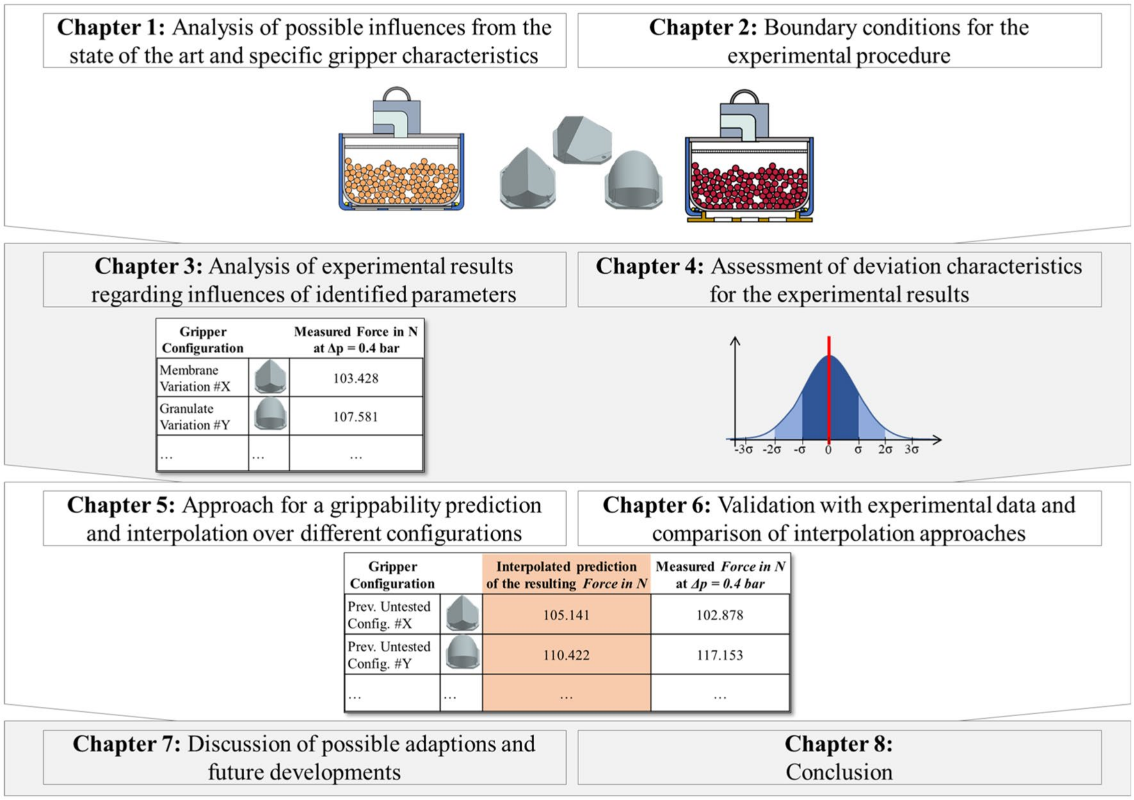

Fig. 3 Overview for the further structure of the following chapters

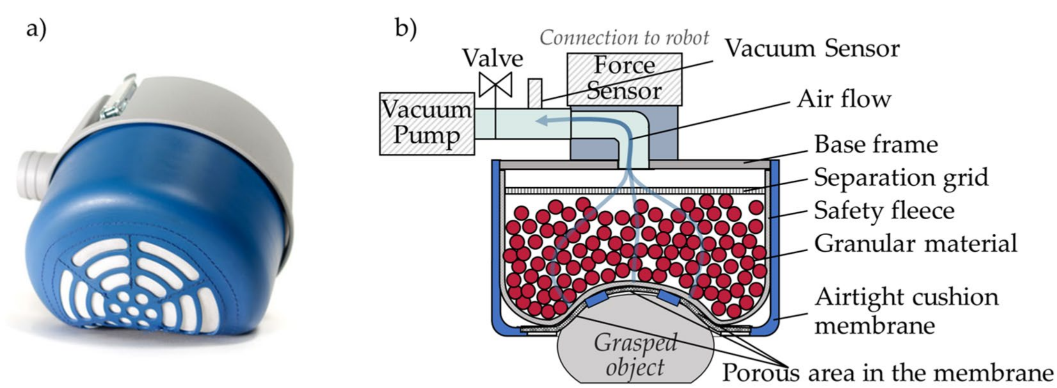

Fig. 4 Overview for the vacuum-based granulate gripper examined in this research: **a** Example for this gripper [37], **b** Schematic of the gripper (based on [16])

resulting grip and is therefore a further influence analyzed in this publication. As noted by previous researchers, individual variations of these characteristics in an experimental manner are somewhat difficult. Due to high costs and low availability, procuring large quantities of homogenously shaped granulate with complex shapes is challenging. Therefore, the granulate shape effects are not investigated further within this publication. Instead, the used granulates are mainly varied regarding **size**, **material** with the dependent roughnesses, weights, air-permeability and elasticities as well as **filling ratio**.

Relevance of membrane variations for the specific examined gripper

In general, the hulls and membranes of granular grippers within the state of the art tend to be of a spherical shape. However, this is not the case for the examined specific gripper. Its strengths in versatility for both convex and concave objects have proven an initially mostly flat porous membrane and therefore a cylindrical shape of the gripper to be most successful. Therefore, the general shape and dimensions of the gripper are not varied within this study.

For the different types of objects, predominantly the porous area at the GOI and its sealing is suggested to influence the gripper's characteristics. For this, the elasticity and stiffness of the membrane material at the GOI as well as the size and arrangement of the permeable zone should be varied in order to determine their influence on the resulting gripping force.

Previous research for the specific examined gripper and experimental boundary conditions

The key distinctive feature for the investigated gripper compared to conventional granular grippers is the porous area in the membrane (see Fig. 2). The gripper is capable of molding to different object surfaces, enabling a seal between the porous areas of the gripper and the gripped object. When a pressure difference is applied and a stable seal is achieved, the granulate jams around the gripped object. Resulting forces from these jamming effects combined with the primarily influential suction force enable a secure grip for a multitude of objects. However, due to the various interacting influences involved, the resulting achievable gripping force varies widely for different gripped geometries. This dependency on object geometry was already discussed in previous research [16] and is briefly summarized in the following paragraphs.

The experimental setup used in previous research is identical to the experiments layed out in the next chapters. The gripped objects are manufactured from Polyactic Acid (PLA), the surface roughnesses and material of objects were found to have a negligible influence with the tested spectrum [16]. The objects are fixed to a surface, while the gripping force is measured using a pull-off test. A gripper with dimensions of 60 mm in height and 150 mm in diameter filled with granulate is utilized. The symmetrically arranged porous area at the bottom of the gripper has a maximum diameter of 95 mm. Within the experimental procedure, both the forces in Z-direction and the vacuum are recorded as shown in Fig. 5. The gripper is connected to a K6D40 force sensor, which is mounted to a Kuka LBR iiwa robot. The air pressure difference is created by a Variair Unit SV201/2 (up to 4 kW), which can create a relative pressure difference of up to 0.42 bar when a valve is opened. This is measured by a VS VP8 SA M8-4 vacuum sensor. Movements within this study are exclusively perpendicular to an objects surface (in Z-direction). The gripping process begins with an initiation of the GOI, which is achieved with an initial contact force of 80 N for this research (see Fig. 5). When the valve from the pump to the gripper is opened, the gripper is pulled vertically upwards at a defined speed after a delay of 2.5 s until it detaches completely from the object surface. The maximum recorded gripping force is used and described in the following paragraphs as the achievable gripping force for an experiment.

As the gripping force of the gripper varies with the applied vacuum, a physical law or relationship between these factors is proposed. This aspect was investigated by Wacker et al. [16] and is comparable to the characteristics of a conventional suction gripper especially for mostly flat surfaces. As long as over 90% of the GOI between the grippers porous area is covered by the object, the

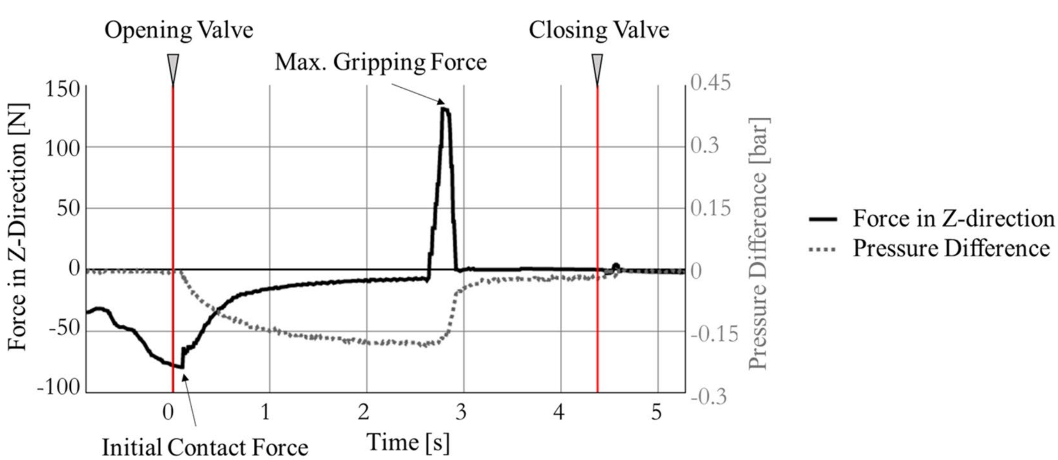

Fig. 5 Overview of the experimental procedure regarding force in Z-direction and pressure difference for an initial contact force of 80 N and 100% compressor power (derived from [16]); images of the gripper deformation are shown in Fig. 27 in the appendix

achievable gripping force $F_{achievable}$ can be approximated as being linear with the applied pressure difference Δp (see Eq. 1).

$$F_{achievable} = C_{combined} \cdot \Delta p \cdot A_{tmax} \quad (1)$$

However, for more complex geometries, both jamming and slip-off-effects influence the seal of the GOI. Therefore, a correction parameter $C_{combined}$ as well as the area A_{tmax} for the combined influences on the gripping force were introduced. The correction parameter $C_{combined}$ is specific to individual object geometries and combines the influences of the affected area with the granular jamming and slip-off-effects. Values of $C_{combined}$ range between 0 and 1. It could be hypothesized, that merely the size the porous area of the gripper determines the maximum gripping force, especially for mostly flat surfaces. However, experimental results have exceeded this calculated force, which is suggested to be a result of airflow effects and curvatures in the membrane areas. These curvatures are characteristic for granulate-based grippers and were previously discussed in Figs. 1 and 2. Therefore, the effective area of the porousity is difficult to gauge and suggested to be also influenced by object geometries. In order to establish an equation, which enables a calculation of the theoretical maximum gripping force, the theoretical maximum effective area for the suction force is used and set to A_{tmax}. This value is defined as the theoretical scenario with the highest achievable suction force, where the entire 150 mm diameter of the gripper curves inward, so that the entire area of the gripper acts as a suction cup gripper. This is set as the limit for the maximum possible gripping force and where the upper limit of $C_{combined}$ is defined at the value of 1. The object-specific parameter $C_{combined}$ is currently determined through experiments. It exhibits a high accuracy to the linearization proven by a high coefficient of determination of up to 0.99 [16]. Exemplary achievable gripping forces over different applied pressure differences are shown in Fig. 6, visible is the mostly linear relation to the pressure difference. The parameter $C_{combined}$ therefore serves as an object-specific characterization of the slope of these linearizations.

In order to include this object-specific dependence of gripping forces, a broad object spectrum with surfaces resembling possible gripped objects should be evaluated. To accomplish this, various basic geometries placed on a 170×170 mm pedestal are used. These geometries exhibit convex and concave rotational and non-rotational symmetric features (see Fig. 7). Theoretically, this dataset could be divided into classifications such as axis- and planar-symmetric objects or various other categories. However, for a reduced complexity and increased comprehensibility, further chapters refer to the three categories of convex, concave and other geometries. Additionally, structured repetitive surfaces are examined. Preliminary experiments for this spectrum of 31 objects have resulted in a wide variety of achievable gripping forces reaching up to 300 N. When converting achievable forces and their respective pressure differences into values for $C_{combined}$, the results range mostly between 0 and 0.5.

A $C_{combined}$ close to zero is achieved for objects with very complex geometries, when the gripper cannot deform and create a seal with the GOI. This limit of gripper deformability is suggested to depend on the gripper configuration.

Experimental procedure

As discussed in chapters 1 and 2, in order to assess their object-specific impact on achievable gripping forces, the granulate parameters as well as membrane parameters should be evaluated. For the specific gripper, especially the porous area of the membrane at the GOI is hypothesized to have the largest influence. Therefore, prototypes for a modular gripper with interchangeable membrane areas for the porous zones were developed. Preliminary experiments have proven effectiveness of the setup shown in Fig. 8b) for a modular

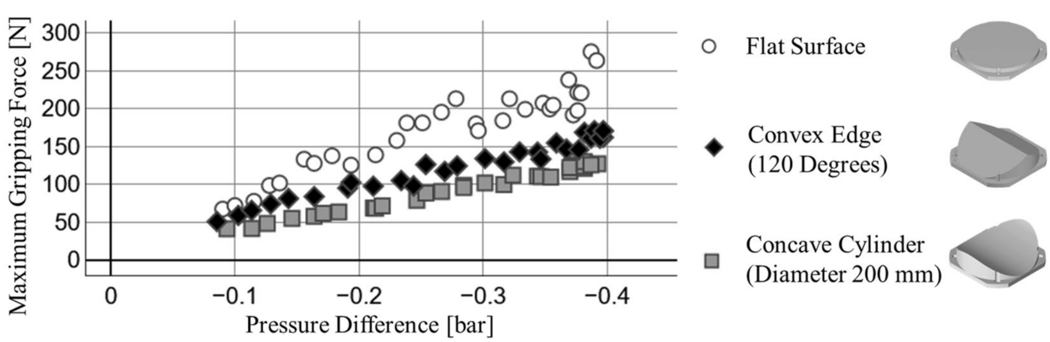

Fig. 6 Exemplary achievable gripping forces for 30 repetitions over a range of pressure differences (30 to 100% of possible compressor power)

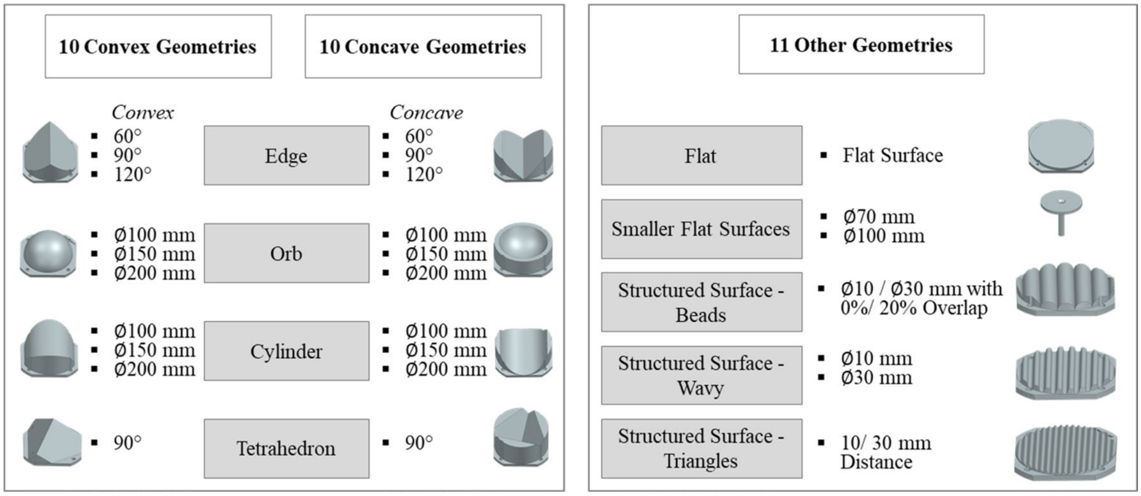

Fig. 7 Overview of the analyzed object geometries, see the appendix (Fig. 28) for further information

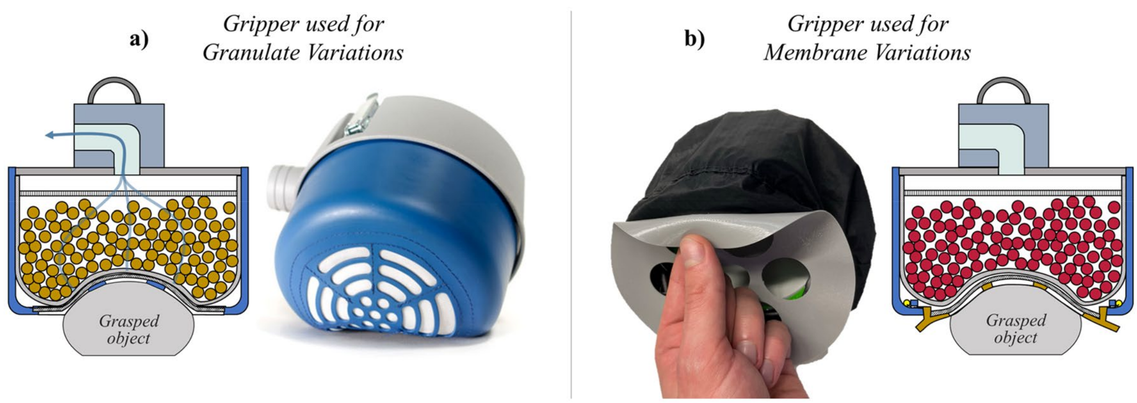

Fig. 8 Grippers examined within this research with **a** Gripper used for granulate variations and **b** Gripper used for different porous zones within the membrane

interchangeability of this porous zone while reducing manufacturing efforts immensely. The key difference between the grippers used for the granulate and membrane experiments is the inclusion of an additional collar in the membrane gripper design, while the remaining aspects of the design, such as dimensions, are retained.

The collar is located at the outer-most rim of the membrane (see Fig. 9), while the inner part can be designed with individually arranged patterns for a desired air permeability at the GOI. The entire modular membrane shown in grey in Fig. 9b) can be replaced while retaining the entire rest of the hull, where the modular membrane is merely sewn in. Thus, manufacturing and material effects of the hull can be excluded as influencing factors for the experiments with different modular membranes. The gripper shown in Fig. 8a) is used for the experiments involving granulate variations, while the gripper

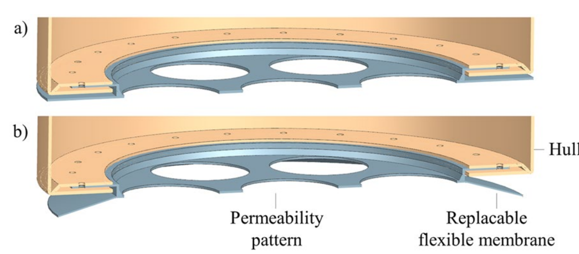

Fig. 9 Gripper used for membrane variations with sections showcasing **a** The idle state of the gripper and **b** The collar's adaptability to an object, similar to a sealing lip

shown in Fig. 8b) is used for the evaluation of membrane variations.

Both types of grippers are tested with the 31 objects introduced in chapter 2 with 15 experiments per object for vacuum pump settings ranging from 50 to 100% of the available power. These 15 data points are used to interpolate $C_{combined}$, which allows for an assessment of achievable gripping forces independent of applied pressure differences. This parameter could also be described as an indicator for the effectiveness of this gripper for a certain surface geometry. In Fig. 10, the resulting gripping capabilities for the investigated objects are compared for the two gripper types in their reference configuration, referred to as standard configurations in the following chapters.

Only objects with a $C_{combined}$ of over 0.15 are classified as grippable, which corresponds to a gripping force of over 114 N when the maximum pressure difference of 0.42 bar available within the experimental setup is applied. This value is established as an example for a possible threshold for a successful grip within the further chapters, but could be adapted individually for specific use cases.

Especially for the objects classified as 'other' geometries, the behavior of the gripper designs is mostly comparable, the gripper used for granular variations even shows some minor advantages for some of these objects. However, the gripper design used for the membrane experiments appears to enable a successful grip for a larger amount of objects as well as a tendency towards increased values for $C_{combined}$ for both concave and some convex geometries. This could be a result of the additional deformability of the collar, which allows for an improved sealing for some geometries. A larger overview of the tested objects and the respective achieved values for $C_{combined}$ for the two standard configurations is available in the appendix (Fig. 28).

Examined materials

As discussed in chapters 1 and 2, the evaluation of granulate materials focuses on size, material and filling ratio. The variations are shown in Fig. 11. The standard

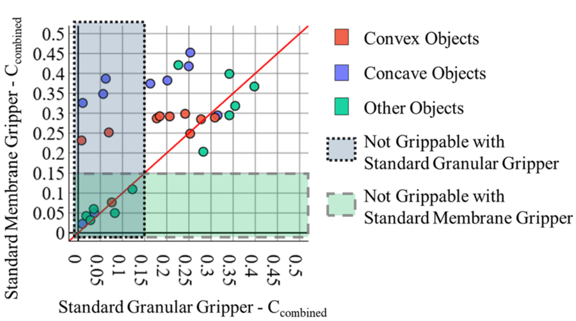

Fig. 10 Comparison of the experimentally determined values for $C_{combined}$ for the objects for both standard configurations of the examined types of grippers, a perfect fit would be on the bisecting red line

granulate setup for the gripper is based on preliminary experiments and consists of a filling with Acrylonitrile Butadiene Styrene (ABS) 6 mm balls with a volume of 66% of the maximum capacity, which is equivalent to 658 cm3. The membrane consists of 1.25 mm thick Polyurethane (PU), where the porous area is arranged symmetrically around the center axis (see Fig. 4) for a total size of the permeable area of approximately 4500 mm2. In order to limit experimental effort, the variations of these parameters are experimentally examined in a one-factor-at-a-time design and later compared regarding a possible interpolation for a full-factorial overview. For instance, the granulate size is experimentally tested with larger and smaller granulate, while keeping the material and the filling level constant as ABS and 66% respectively. The granulate material is varied over a larger spectrum, as preliminary research has shown various effects, which are challenging to isolate individually. As an example, the surface characteristics of the granulate material might have an influence on the jamming effect, similarly, the elasticity of granulate material could inhibit material flow-effects or influence curvature effects of the membrane. Therefore, a variety of materials are used, including a second ABS granulate with a comparable surface, but increased weight and reduced elasticity. Steel granulate, characterized by its heavy weight, smoother surface and a comparably higher E-Module, is also tested. This is in contrast to the silicone materials, which are elastic with increased friction compared to steel. Additionally, a 3D-printed Polyethylene Terephthalate (PET) granulate is examined, which exhibits a structured surface resulting from the employed Fused Deposition Modelling (FDM) process. This structured surface could affect the granulate movements as well as the jamming behavior. Moreover, considering the gripper's specific air-flow effects, the printed granulate is additionally examined as a hollow air-permeable variant, as seen in Fig. 11. Furthermore, a hollow brass granulate exhibiting a smoother surface and higher weight is evaluated. The granulate filling level is varied over five different steps, as some influences were visible during preliminary experiments.

The membrane variations are depicted in Fig. 12. Similar to the granulate variations, only one factor is varied at a time, while the other parameters are kept at a constant value. The granulate material, size, filling as well as the standard size of the permeable area (*permeability*), which makes up approximately 50% of the possibly permeable membrane area identical to the standard configuration of the granulate variation. The standard configuration for membrane variations therefore closely resembles the gripper used for the granulate variation; however, it is differentiated through a collared membrane. The rest of the gripper hull consists of a PU-coated nylon for all

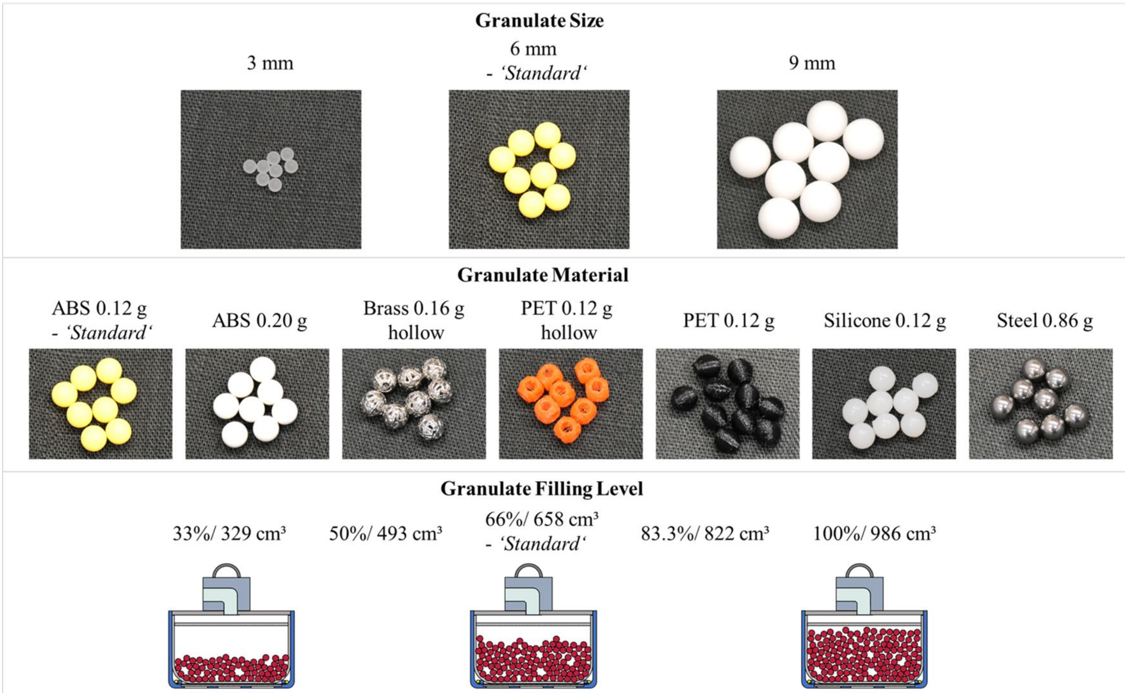

Fig. 11 Overview of the granulate variations examined within this research, further information is available in the appendix (see Fig. 32) and the supplementary material

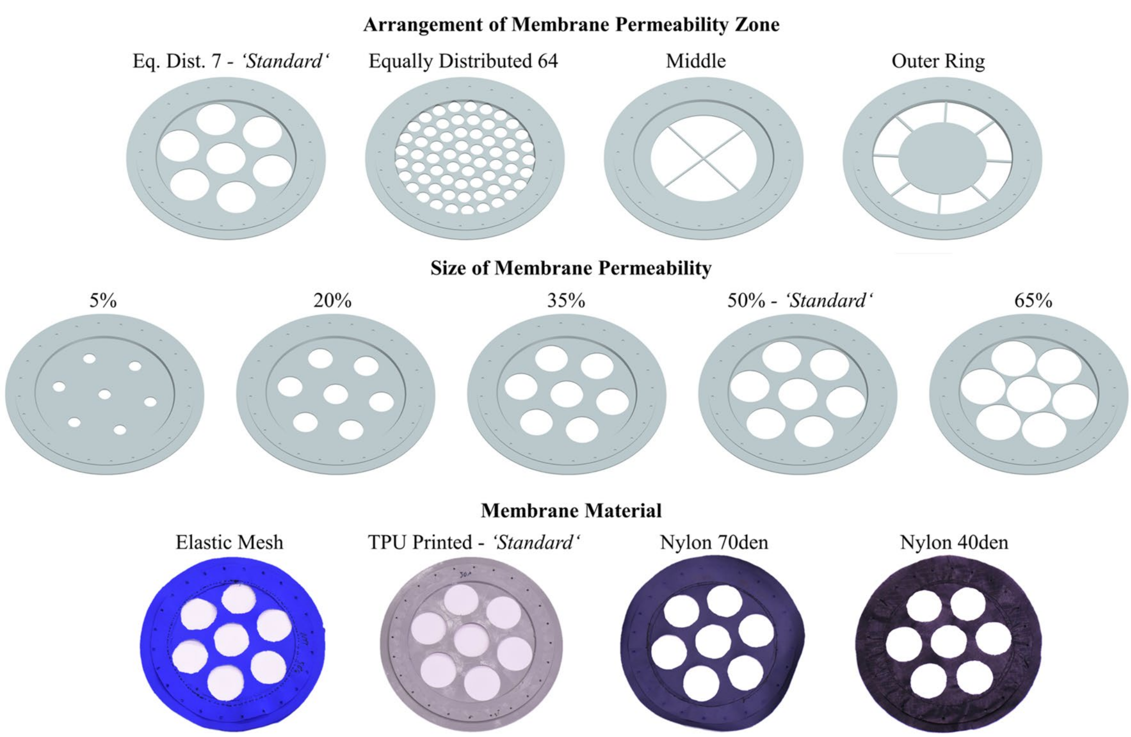

Fig. 12 Overview of the membrane variations examined within this research, further information is available in the appendix (see Fig. 32) and the supplementary material

experiments with this gripper design. The replaceable collared membrane is FDM-printed from 85 A thermoplastic polyurethane (TPU) with seven equally distributed holes for a defined size of the air-permeable area within the GOI as the standard configuration. By utilizing 3D-printing technology, various arrangements and sizes of the permeability zones can be easily designed and printed, eliminating the need to examine manufacturing inaccuracies when manually cutting elastic membranes. Influences impacting the curvature behavior of the membranes might stem from the size of the areas, therefore different equally distributed zones with different sizes are investigated (see *Equally Distributed 7* or *64* in Fig. 12). Additionally, the specific locations of these zones might influence the grippability of different object types (see *Middle* or *Outer Ring* in Fig. 12). The size of the permeability area was varied from 50% mostly to lower values, aiming to highlight possible correlations between a reduced permeability size and resulting achievable gripping forces. Values above 65% were not examined, as a differentiation between zone arrangements would be difficult to implement. Regarding the membrane materials, two different stiffnesses of PU-coated nylon were evaluated, along with a comparably more elastic PU-coated mesh.

Some parameters such as granulate size, granulate volume or size of the membrane permeability could be considered as continuously variable parameters and interpolated between the examined values. For an increased comprehensibility of this research, these parameters are simplified as discrete steps.

As previously mentioned, a total of 15 experiments were carried out for each tested gripper configuration using all 31 examined objects. As summarized in Fig. 13 II, this results in $31 \times 13 = 403$ values of $C_{combined}$ for the granulate variations as well as $31 \times 11 = 341$ values of $C_{combined}$ for the membrane variations. Achieving individual full-factorial results for each examined gripper (Fig. 13 III) would enable estimations for 105 different granulate configurations for the 31 objects as well as 80 interpolated membrane variations. Theoretically, these configurations could be combined for an interpolation encompassing both gripper types, yielding a total of 8400 different configuration setups. This would allow for estimations for all 31 objects, resulting in $31 \times 8400 = 26{,}040$ values of $C_{combined}$.

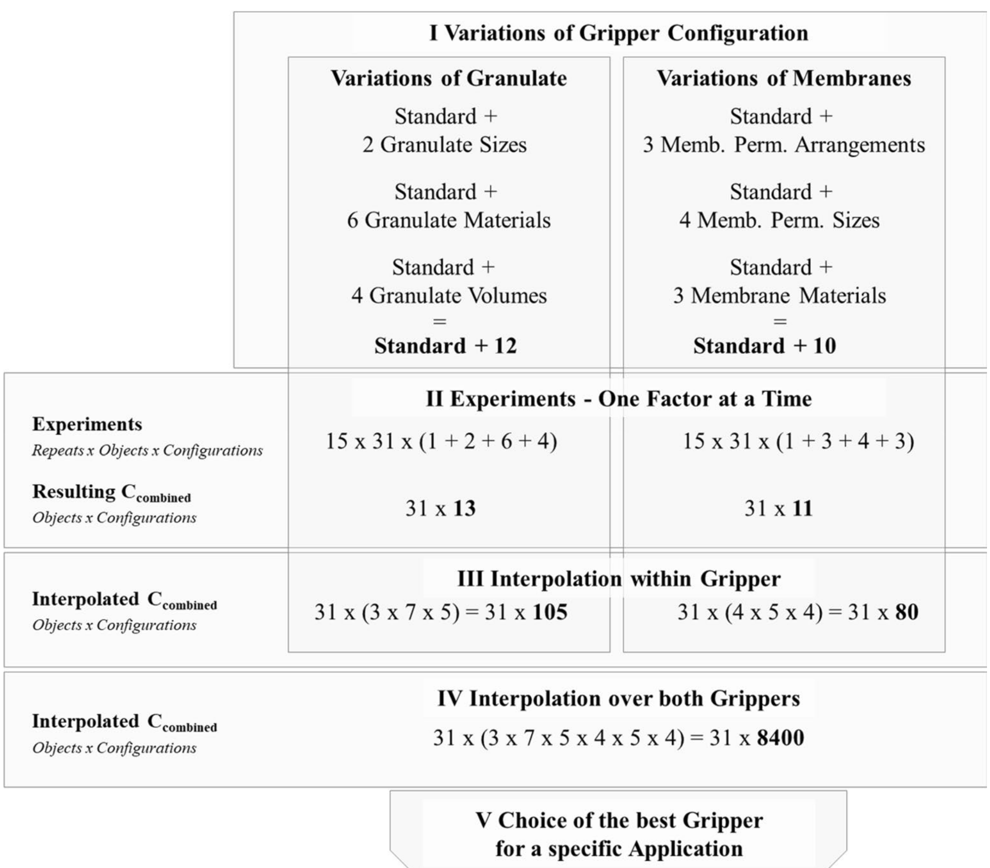

Fig. 13 Overview of the experimental procedure and analysis for the different gripper configurations

However, many of these configurations might not exhibit large characteristic differences in their achievable gripping forces and have to be examined regarding its influence. Similarly, some configurations could merely be very successful for specific object types, such as only concave or convex objects, while being unsuitable for other object types. In order to enable an overview of the different configuration influences and provide a basis for a future choice between gripper configurations, the results and influences of the examined parameters are presented within the next chapter.

Results and influences of the parameters

The results for the one-factor-at-a-time experiments are shown, exemplary for the granulate size, in Fig. 14. Detailed results for all other experiments are available in the appendix in Fig. 29. Similar to previous depictions (such as Fig. 10), only objects with resulting values of $C_{combined}$ above 0.15 are shown, representing the threshold for a grippability within this study. In addition, a small overview for all varied parameters is included, providing the number of grippable objects exceeding a difference of $C_{combined}$ (Δ to Standard) of over 20% compared to the respective standard configuration. In order to enhance the comprehensibility of these values, the recorded deviations are not shown and can be accessed within the supplementary material.

In the following sections, the influences on the achievable gripping forces resulting from the variations of the selected parameters are discussed with a focus on the different object spectrums convex, concave and other.

Granulate size

Compared to the state of the art for conventional granular grippers, the impact of the granulate size on the gripping performance is limited for the specific variation examined within this publication. For all three examined diameters, a total of 16 out of the 31 tested objects are classified as grippable. For both the 3 mm and 9 mm granulate size, only one out of the 31 tested objects exhibits an increase for $C_{combined}$ of over 20% compared to the standard configuration (Orb 200 mm concave and Orb 150 mm concave, respectively). Some smaller influences are visible within the histogram for 3 mm, as no values exceed a $C_{combined}$ of 0.35, instead an accumulation of values between 0.3 and 0.325 is visible. The results larger than 0.325 for 6 and 9 mm mostly occur for structured surfaces. A possible cause for the smaller 3 mm granulate being less suitable for these objects, could be a result of smaller orbs being able to move more easily even during compaction, which reduces the molding of the membrane with the structured surface and therefore weakens the sealing and the gripping force.

Therefore, under specific circumstances with a known, reduced object spectrum of the specific structured surfaces, the overall applicability of the gripper could benefit from using granulate material with larger sizes in order to achieve a higher $C_{combined}$; however, this requires knowledge about the handled geometries.

Granulate material

Similarly, the granulate material shows no large deviations for the number of grippable objects. Compared to the standard granulate, the slightly heavier ABS 0.2 g as well as all types of printed and air-permeable

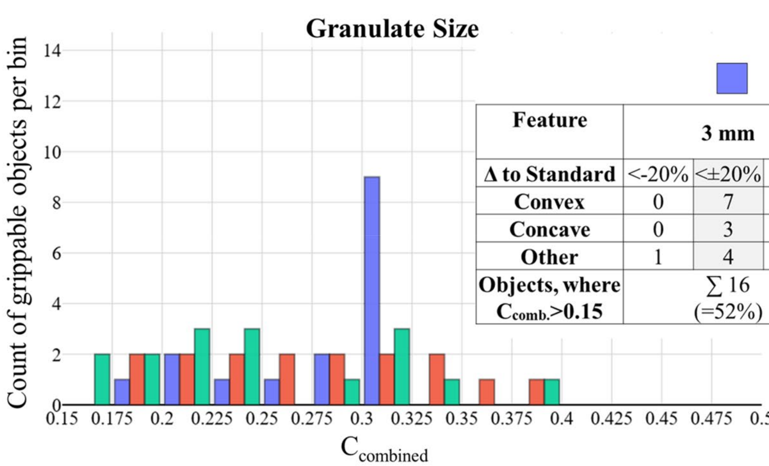

Feature	3 mm			6 mm	9 mm		
Δ to Standard	<-20%	<±20%	>20%	Standard	<-20%	<±20%	>20%
Convex	0	7	0	7	3	4	0
Concave	0	3	1	4	0	3	1
Other	1	4	0	5	0	5	0
Objects, where $C_{comb.}>0.15$	∑ 16 (=52%)			∑ 16 (=52%)	∑ 16 (=52%)		

Fig. 14 Overview of the results for the variation of granulate size differing from the standard (marked in blue), with a focus on objects surpassing a value for $C_{combined}$ of 0.15 and any experiment surpassing 100 N. Similar graphs for all other varied parameters as well as overviews for individual objects (Fig. 30/31) are available in the appendix

hollow granulate appear to have limited effect on the resulting gripping forces, with some improvements for convex and concave geometries. Silicone and steel are the more atypical materials in regards to their elasticity, surface or weight and exhibit the largest visible effects for the materials. Here, steel appears to be specifically beneficial for convex geometries, while silicone achieved some of the highest recorded values for $C_{combined}$ above 0.45 for a small selection of mostly flat objects. Similar effects for very elastic granulate materials were found for other granular grippers within the state of the art [32], effects for steel granulate appear to be especially relevant for the examined specific type of gripper. Notably, these effects do not occur over the entire tested spectrum of objects within this study. The positive influences of the steel granulate might be a result of the increased weight, which enables an overall improved forming of the gripper cushion to some object geometries and strengthens the seal at the outermost borders. For the silicone granulate, the increased elasticity and deformability likely improves the seal and decreases the porosity within the granulate, which has positive effects on the achievable grasping force.

Filling ratio

Among the examined granulate parameters within this study, the granulate volume used to fill the gripper appears to have the largest influence. Especially the far ends of the examined scale significantly reduce the grippability of large amounts of the tested objects. Results for 50% and 82% exhibit some minor improvements and deteriorations for the number of grippable objects as well as specific types of shapes. These findings suggest a potential in fine-tuning the granulate volume, which could be optimized for specific types of objects.

Arrangement of the membrane permeability zone

The shape and design of the membrane permeability zone arrangement exhibits limited influence within the examined spectrum. A design oriented towards an arrangement of the permeability in the middle of the gripper shows some advantages for concave objects. This could be due to the combination of curvature effects of the membrane with the concave object shapes creating an enlargened 'bubble' of enclosed pressure difference. Similarly, permeability zones with smaller diameters exhibited some minor increases and decreases for some objects and could be implemented as possible variations for a fine-tuning of the gripper configuration. The arrangements as an outer ring show no advantages.

Size of the membrane permeability zone

The size of the permeability zone does not appear to majorly affect the resulting achievable gripping forces. When reducing the size of the permeability from 50% down to 5%, some objects are no longer grippable. However, an increase in the achievable gripping force is visible for individual objects in spite of this strongly reduced value for the size of the permeability. Especially regarding concave objects, this is suggested to be a result of the curvature effects. When increasing the permeability size, the number of objects with a value for $C_{combined}$ of over 0.15 shrinks, an advantage for specific objects is not discernible. It would be advisable to include this parameter for fine-tuning the grippers design.

Membrane material

The results obtained from the membrane material demonstrate large variations. The TPU-printed membrane is characterized by the highest stiffness of the examined materials and is the only material achieving values for $C_{combined}$ of over 0.325. This is possibly a result of a correlation between the curvature effects and the stiffness of the membrane material. However, the elastic mesh enables a successful grip for the largest number of objects within the examined configuration spectrum with some increases and decreases for different gripped geometries. The stiffness differences between the PU-coated nylon-materials appear to result in merely minor differences in the number of grippable objects. Based on these observations, it is highly suggestible to include the membrane material as a further influencing parameter for fine-tuning the gripper design for an optimized performance.

Summary of the influences of the examined parameters

As a summary of the results, an overview is shown in Table 3.

The configurations with the slightly heavier ABS 0.2 g, the 'Middle' arrangement for the permeability zone and a membrane permeability size of 65% are the only three tested configurations with no visible advantages. All other tested configurations show up to 4 objects, where an increased $C_{combined}$ of over 20% compared to its 'standard configuration' could be found for values above 0.15.

Deviation characteristics

Enabling an assessment of the achievable gripping force resulting from the selected configuration is one objective of this publication. However, as already elaborated in the state of the art, it is important to acknowledge, that most conventional granular grippers exhibit a large distribution and therefore a substantial standard deviation of achievable gripping forces even when repeated under

Table 3 Overview of influences on the grippability

Parameter	Influence	Comments
Granulate Size	Limited influence	Larger values for $C_{combined}$ are possible merely with larger granulate
Granulate Material	Major influence only for silicone and steel granulate	Effects are only visible for a small spectrum of objects
Granulate Volume	Major influence	Especially the far ends of the filling ratios are only viable for a small number of objects
Arrangement of the Membrane Perm. Zone	Limited influence	Especially an arrangement in an outer ring appears unadvisable
Size of the Membrane Perm. Zone	Limited influence	No direct correlations between size of permeability zone and achievable gripping force are determinable
Membrane Material	Major influence	Varying advantages of elastic and stiff membrane materials are discernible

very similar experimental conditions. During the procedure for the specific gripper examined here, a resulting gripping force was recorded for every experiment and varies within a small range, therefore a direct differentiation between a successful or failed grasp is not possible. This increases the relevance of an examination of the deviation characteristics of the gripper behavior, as a successful grasp is therefore mostly dependent on the mass of the grasped object and the statistical behavior of the gripping force with the respective deviation characteristics.

This deviation of gripping forces is primarily a result of the randomly distributed granulate material within the gripper, which does not behave similarly for every repetition. This statistical distribution of the achievable gripping force for repeated experiments is examined in the following paragraphs.

Normal distribution of achievable gripping forces for repeated experiments

In general, when predicting a value, it is customary to also provide a standard deviation, which enables a statistically meaningful statement about the result. Thus, as long as a normal distribution can be assumed for the gripping force, a calculation of a gripping success could be expressed using standardized methods such as a t-test. This was examined exemplary for the standard configurations of both gripper types used for granulate as well as membrane variations with 15 repetitions. Tests for the examination of data points for a type of distribution usually merely allow to rule out a certain type of distribution with a defined certainty. One such test is the Shapiro–Wilk-test, which can be used to rule out normal distribution and can be implemented for smaller sample sizes. Applying this test to the already presented experiments for the standard configurations, a normal distribution cannot be ruled out for most objects for an alpha of 0.05 (29/ 31 objects for the granulate variation and 25/ 31 objects for the membrane variation gripper). Therefore, based on these individual sample sizes of 15 experiments conducted at different vacuum settings, it is reasonable to assume a normal distribution for the majority of the experiments, although the sample size is relatively small.

To provide a more detailed statement about the deviations for different gripping forces, additional experimental data is presented for 50 repetitions conducted with identical compressor settings and equal experimental parameters (see Fig. 15) for the standard configuration for granulate variations. In these extended experiments, the statistical description of the results appears to be mostly feasible as normal distributions. As the vacuum slightly varies with the achieved seal, the x-axis is chosen as the individually calculated values for $C_{combined}$, thereby displaying the results for the achievable gripping forces in relation to the achieved individual vacuum.

Influences of different objects and pressure differences on the distribution of achievable gripping forces

The deviations tend to increase for larger values of $C_{combined}$, which merely depend on the object shapes in Fig. 15. When performing further evaluations for a dependency between the gripping force and the influencing pressure difference, a phenomenon similar to heteroskedasticity can be determined. Heteroskedasticity refers to the deviation correlating with the examined parameter [38], as seen in Fig. 16a) for 84 repetitions with 7 different compressor settings ranging from 25 to 100%, the deviation increases with the applied pressure difference. Additionally, the collar-effects of the membrane variation gripper appears to require a minimum pressure difference in order to effectively seal the objects surface for more complex geometries such as convex edges, as seen at around 0.18 bar in Fig. 16).

As assessed in Fig. 16, there appears to be an interrelation for at least some objects between the deviation and the resulting gripping force, which is also dependent on the applied pressure difference. Summarizing the results from Fig. 15 and 16, the distribution of

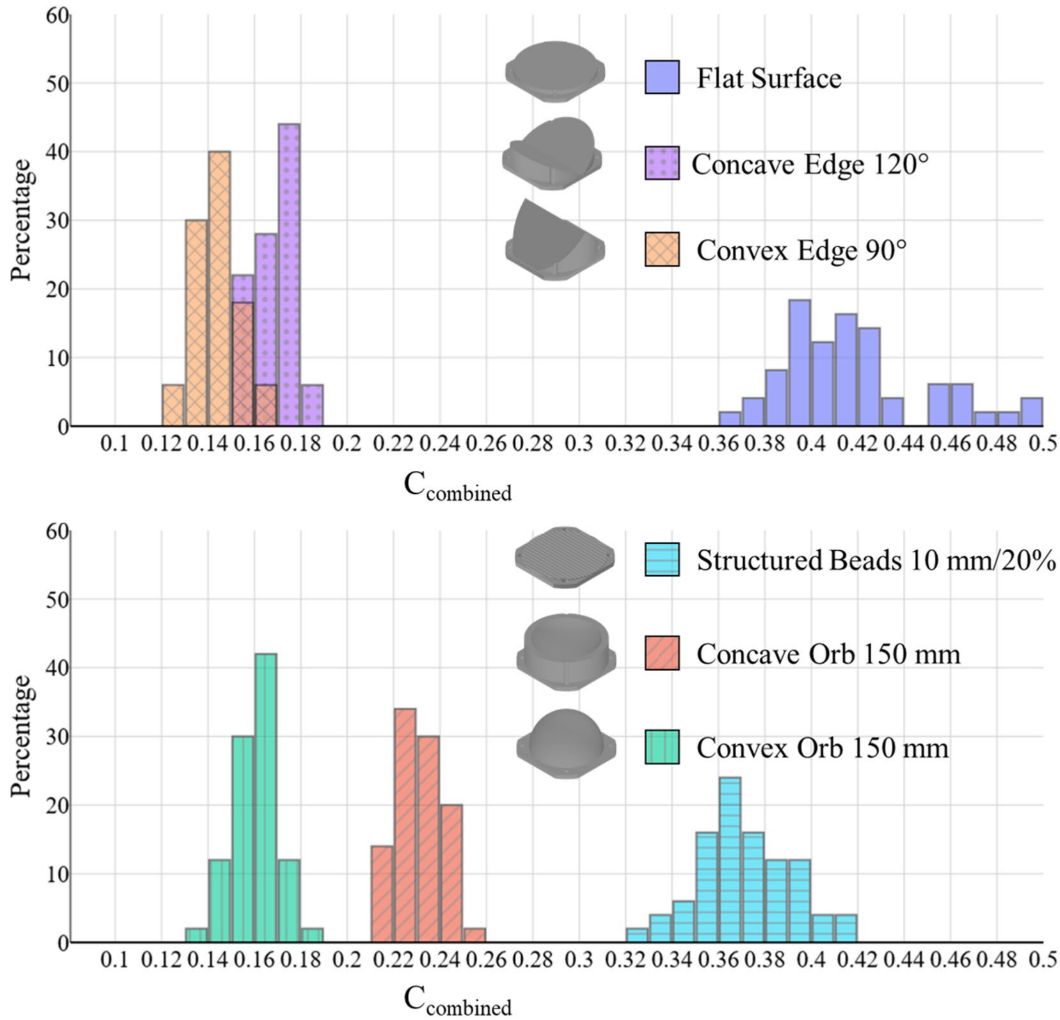

Fig. 15 Exemplary results for 50 repetitions for an initial contact force of 75 N at 50% power for the standard configuration of the granulate variation gripper

achievable gripping forces appears to correlate to both the object-specific gripping force as well as the applied pressure difference. This could be simplified as a correlation of the standard deviation with the individually achievable gripping force itself, which in turn is a result of the specific object surface and pressure difference. As the value $C_{combined}$ enables an object-specific prediction of the achievable gripping force with a defined pressure difference, an abstraction of the standard deviation as a percentage of $C_{combined}$ would achieve an integration of both the interrelations with the object geometry and the pressure difference. In order to facilitate this, the experimental data for the configuration variations of both grippers is examined for possible correlations on the standard deviation within the values used to determine the individual values for $C_{combined}$.

In order to present a comprehensive overview, it is necessary to exclude values below a certain threshold when plotting the standard deviation as a percentage of the approximated value of $C_{combined}$. This exclusion is important to prevent objects with a negligible gripping forces and high variations, such as those around 0 N with variations of up to 2 N, from skewing the overview. Therefore, Fig. 17 displays the objects with values above the previously discussed threshold of $C_{combined} = 0.15$ for the standard settings of the experimental setup for all experiments for both granulate and membrane variations. In addition to the proportion of the relative standard deviation for the experiments in the upper graphs, a negative cumulative plot of the relative standard deviation is shown below. With these graphs, it is possible to approximate the relative standard deviation, which peaks within the relative count for both types of grippers at around

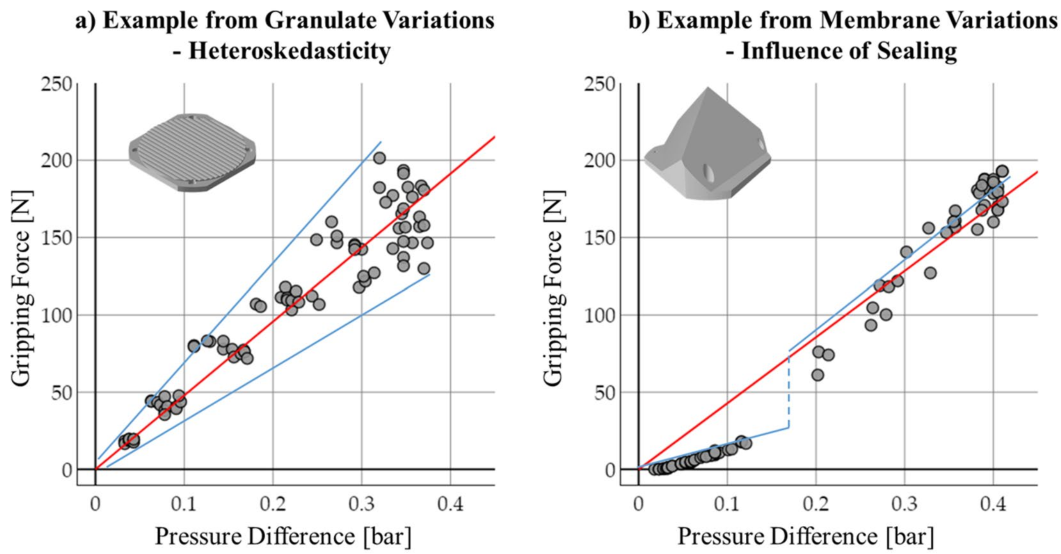

Fig. 16 Influences (traced in blue) on the achievable gripping forces related to the applied pressure difference, the red line resembles the calculated achievable gripping force with the factor $C_{combined}$. **a** For the influence on deviations exemplary for the standard configuration of the gripper used for granulate variations for the object 'structured beads 10 mm/ 20%' and **b** For the influence on sealing exemplary for the standard configuration of the gripper used for membrane variations for the object 'tetrahedron convex'

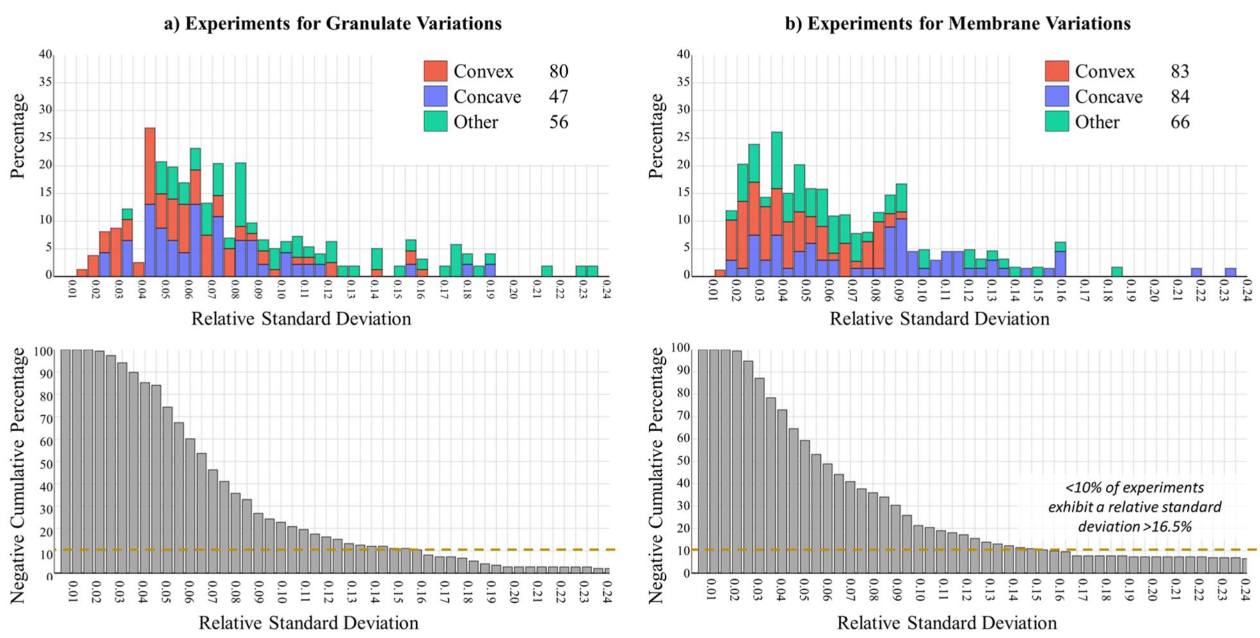

Fig. 17 Overview of relative standard deviation for both examined types of grippers to approximate an overall relative standard deviation

5% (upper part of Fig. 17). However, in order to enable a generalization for most available data points, an assumed relative standard deviation of 16.5% would exclude less than 10% of the remaining experiments (see Fig. 17 lower part). To further enhance the level of confidence in achieving a successful grip, larger values for the relative standard deviation could be considered in accordance with this graphic. Additionally, if required, a simplification for a type of object such as convex or concave could be made when applicable to a specific use case.

As a possible example, the relative standard deviation for convex objects within the hull experiments did not exceed 10% (see Fig. 17), which could be a possible simplification if the object spectrum of a given application exclusively consists of convex objects. Based on the available information known at this point, it can be assumed, that this relative standard deviation applies to any configuration of the examined grippers for pressure differences over 0.2 bar. This knowledge provides valuable guidance for selecting appropriate gripper configurations and process parameters with an orientation value for a standard deviation for any gripper configuration.

Approach for a grippability prediction and the selection of the most suitable configuration

The information obtained from the analysis of the gripper's behavior in relation to design and object shape, as presented in chapters 2–4, coupled with the availability of a standard deviation estimation (chapter 4) enables the derivation of general approaches for the practical application of this gripper. In order to predict a grippability or success rate of an object in a real use case, the following methodology is proposed:

1. Generation of a prediction of the values for $C_{combined}$ for all examined objects for all interpolatable configurations
   - This can be achieved through interpolating the experiments from chapter 3, which enables a prediction of achievable gripping forces independent of the selected pressure difference
2. Determination of process requirements
   - Object shapes and required gripping forces based on object weights, accelerations and safety factors
3. Selecting the applicable most similar object shapes from the spectrum of known objects
   - Definition of the spectrum of gripped shapes, such as 'only convex geometries'
4. Selecting a statistical certainty for a gripping success
   - Specify the desired level of confidence (such as 95%) using statistical tests such as the t-test, along with the relative standard deviation determined in chapter 4
5. Filtering the predicted values for $C_{combined}$ for configurations achieving the process requirements
   - Enables a list of gripper configurations capable of achieving the necessary certainty of a secure grip of the examined object spectrum
6. Optional: Integrate additional criteria and further filtering
   - Possible criteria could be cost, durability or availability of gripper materials
7. Selecting the gripper configuration with the highest overall minimum certainty over the selected object spectrum as the best possible option within the examined scenario
   - The minimum certainty of the examined objects would have the highest chance of a failed grip and therefore represents the 'weakest link' of the filtered configurations.
8. If required, further fine-tuning with additional experiments

As the first step, the prediction of values for $C_{combined}$ requires a modeling of an interpolation between the presented experiments, which were performed in a one-factor-at-a-time design. To enable an assessment of achievable gripping forces for grippers with simultaneous variations of multiple parameters, different approaches for full-factorial interpolation methods are investigated. As previous studies for conventional granular grippers suggested no major interrelations between influencing parameters of the gripper configuration [25], the differences in accuracy of linear and more complex interpolations is of interest and examined in the following. Therefore, two methodologies for a linear interpolation and an interpolation based on Machine Learning (ML) are applied and compared.

Linear interpolation

The first and more basic methodology is the linear interpolation of values within the gripper types. When interpolating between the gripper types, either a relative or an absolute linearity can be considered. For instance, using a granulate size of 3 mm instead of the standard 6 mm for the convex edge with a 90° angle, a corresponding increase for $C_{combined}$ of 0.00856 is observed, which is equal to around 4.65% compared to the standard value. In the case of gripper used for membrane variations, no experimental data regarding the influence of granulate size was evaluated. It would therefore be possible to either assume an absolute increase of 0.00856, or a relative increase of 4.65% compared to the value for the changed base of reference with the standard gripper for membrane variations. This differentiation between absolute and relative linear modelling only applies to parameters not used for the initial determination of this difference. Therefore this differentiation is made for interpolating between the two examined gripper types.

Interpolation based on machine learning

Another methodology is the inclusion of methodologies based on Machine Learning (ML). ML methods have gained popularity for interpolating data over multiple experiments with a limited sample size. While linear or polynomial regression can be used for interpolation, ML-based methodologies offer the flexibility to include various parameters and can therefore model complex behaviors. Various parameters can be included with limited effort for the model-free ML-based interpolation. Using ML-based interpolation would enable a continuous integration of further experiments; however, these types of methods are often less transparent for end users [39–41].

For the following chapters, an Artificial Neural Network (ANN) is compared to the linear interpolation. For this, a One-Hot-Multilayer-Perceptron network based on the keras framework for python is used. In this approach, the input information is coded as true or false values (see Fig. 18), while the output is the resulting value for $C_{combined}$.

This approach employed a quadratic-shaped perceptron network to perform the interpolation. The hyperparameters of the network were trained using a grid search consisting of 2000 variations. This resulted in approximately 90 neurons for both hidden layers using a Rectified Linear Unit (ReLU) activation with a dense sequential implementation using the 'adam' optimizer. Additionally, possibly negative predictions for $C_{combined}$ were set to 0 to remove unrealistic errors. The described approach was repeated for a prediction for both gripper-specific interpolations as well as an overarching interpolation between both grippers in accordance with Fig. 13 (chapter 2).

Experimental validation of prediction approaches

The accuracy of a prediction with the absolute and relative linear interpolations as well as a ML-based prediction is further evaluated and validated in the following paragraphs. This validation is conducted by comparing predicted values from the different presented interpolation methods with experimentally determined values for $C_{combined}$. This was performed for a selection of previously untested combinations of gripper configurations, which were selected based on high overall gripping forces over many different objects. The experiments used to generate the validation of the predictions were carried out in the same manner as the training data.

As two different types of grippers are examined (see Fig. 19), the following paragraphs start with a validation of a prediction within the individual gripper types, followed by a more extensive overview of predictions across both types of grippers. Especially the different base line (standard values for each gripper) of different achievable gripping forces regarding a grippability of objects could influence the applicability of the examined predictions, as the standard gripper for membrane variations already enables higher values for $C_{combined}$ for a number of objects within the examined object set.

Prediction within singular types of grippers

The iprediction of gripping forces for the exclusively granulate variations is validated through an experiment

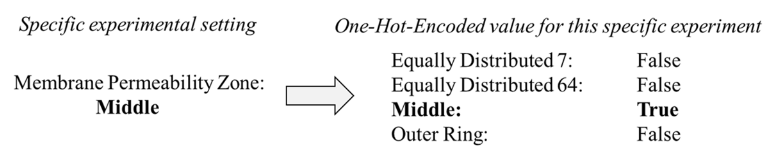

Fig. 18 Example for the input for One-Hot-Encoding for the arrangement of the membrane permeability zone

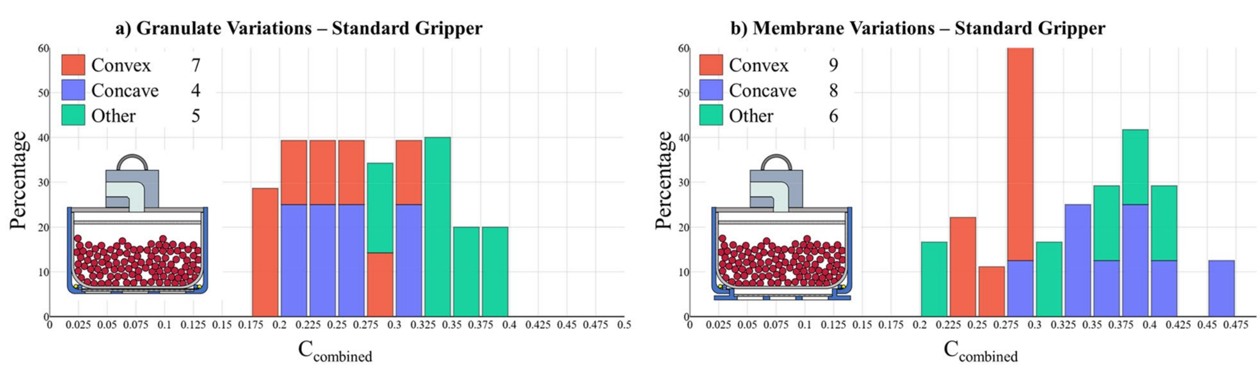

Fig. 19 Relative frequency of values for $C_{combined}$ over 0.15 for the standard configurations. **a** For the gripper used for granulate variations as well as **b** For the gripper type used for membrane variations.

within the gripper variation used for granulate variations (see the configuration specified in Fig. 20). In this case, the membrane parameters could not be varied, as the non-modular variant of the gripper without the collar functionality was used. As the same reference system is used for the relative and absolute linear model, they cannot be distinguished for this experiment. Illustrated are the predicted interpolated values for $C_{combined}$ over the experimentally measured values. To quantify the accuracy of the predictions, the Root Mean Square Error (RMSE) is used, which provides a rough estimation of the average error between the fitted predictions for all examined objects. In order to improve the comprehensibility, the RMSE is shown for the conversion of $C_{combined}$ into the achievable gripping force at an applied pressure difference of 0.42 bar, the maximum value within the examined experimental setup. The linear model exhibits lower accuracies for 'other' geometries with an RMSE of 80.35 N for this classification of object, where the predicted values are primarily lower than the experimentally determined values. The other classifications of objects 'convex' (RMSE of 53.72 N) and 'concave' (RMSE of 42.66 N) are more accurately predicted with the linear model. However, the highest accuracy was achieved for an ANN trained specifically for the singular type of gripper. Despite having the same input as the linear model, the ML approaches appear to dampen the inaccuracies of the linear interpolation, which supports a not completely linear interaction of the configuration parameters.

Analogue to the previous paragraph, Fig. 21 shows the comparison with experimental results for an exemplary configuration solely for a membrane variation. The granulate used is the standard filling for both types of grippers.

In terms of prediction quality, it is observed, that the concave cylinder with a diameter of 100 mm poses a challenge for all methodologies, as evidenced by the blue outlier at the experimental $C_{combined}$ value of 0.25.

For other objects, the prediction accuracy for ANNs trained for a single gripper continues to be more accurate compared to the linear model or the ANN trained for both grippers. Both configurations within a singular gripper show similar overall achievable accuracies (see Figs. 20 and 21), which support a general feasibility of a prediction of configuration parameters. However, the ML-based approaches, which are capable of modeling non-linear influences, achieve the highest accuracies. This emphasizes possible interactions between the influencing parameters, which cannot be entirely represented with the linear model.

Prediction over both types of grippers

In addition to the interpolation within a singular gripper type, an overarching application of adjusted parameter settings for both granulate and membrane influences is examined for a variety of configurations. For this purpose, the gripper for membrane variations is used, as this enables a modular reconfiguration for both types of influences. Figure 22 shows a modification of only the granulate material with an otherwise standard gripper used for membrane variations.

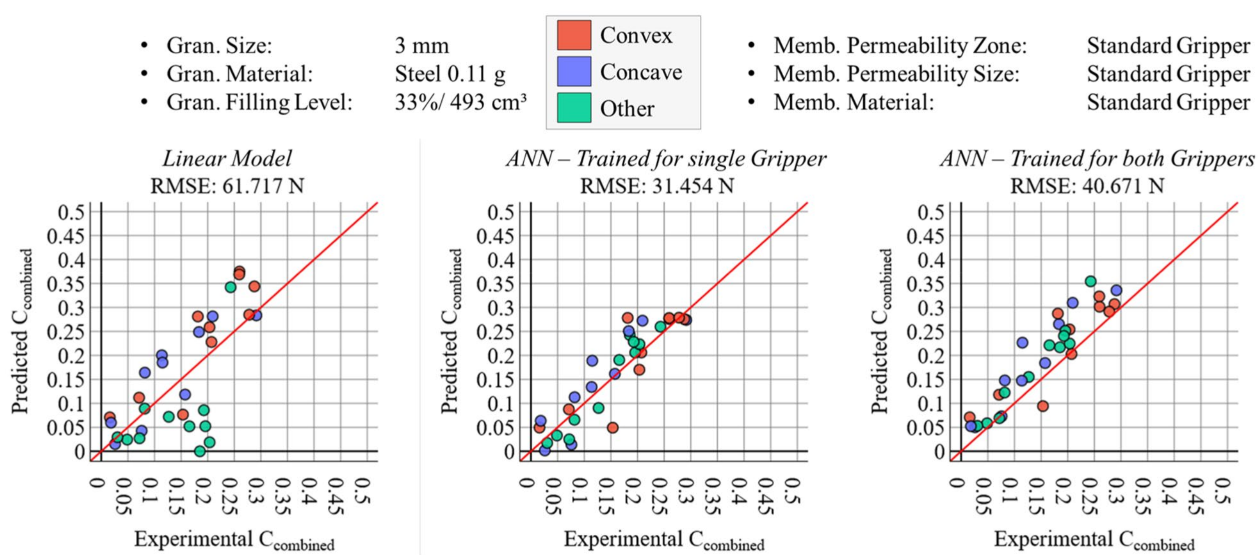

Fig. 20 Prediction within the gripper type used for granulate variations with different values for size, material and filling level compared to the standard configuration, a perfect fit would be on the bisecting red line

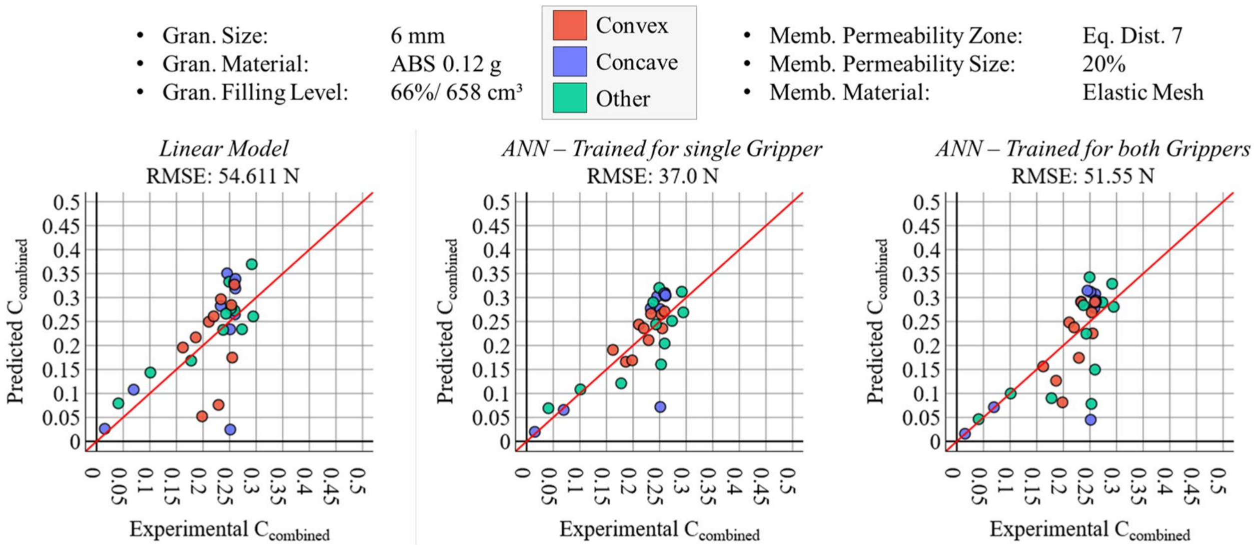

Fig. 21 Prediction within the gripper type used for membrane variations, a perfect fit would be on the bisecting red line

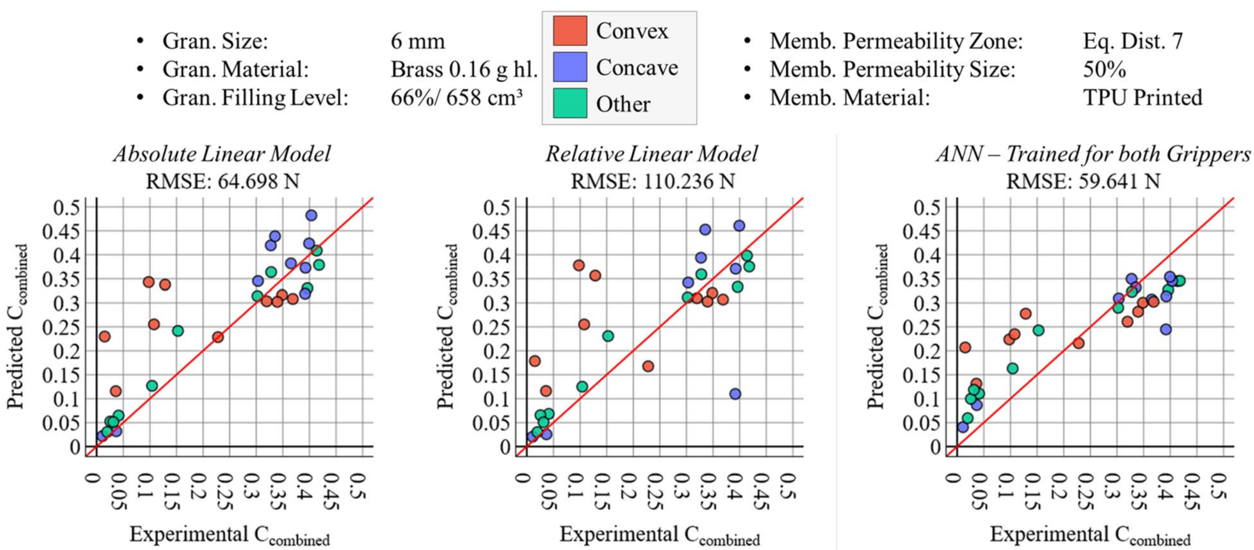

Fig. 22 Prediction of an adjusted granulate material within the gripper type used for membrane variations, a perfect fit would be on the bisecting red line

For this configuration, the ANN trained to a singular gripper is not applicable, as the reference system is now used across both types of grippers. However, the absolute and relative linear model can be differentiated, with the relative interpolation displaying comparably worse accuracy. The differences in achievable gripping forces of object geometries between the two gripper types therefore do not appear to benefit from an approximation as a purely relative influence. The ANN-based prediction is slightly more accurate compared to the absolute linear model.

The experimental results for a larger amount of varied parameters are shown in Fig. 23 and demonstrate similar accuracy differences. The absolute linear model appears to be distributed around a perfect fit for low and high values of $C_{combined}$, while the data points for the ANN are mostly spread out for higher values. A number of outliers are visible for the prediction with

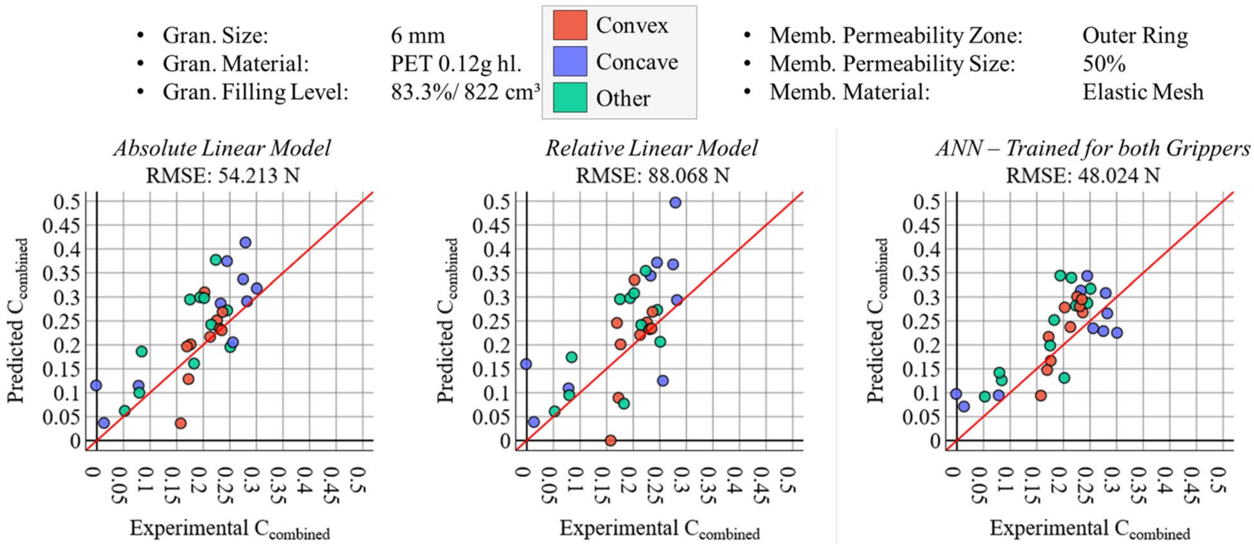

Fig. 23 Prediction of varied granulate parameters within a variation of the gripper type used for membrane variations, a perfect fit would be on the bisecting red line

the relative linear model, for all classifications of examined objects. In general, the results reinforce the best fit for ANN-based interpolations followed by absolute linear models, with the relative models resulting in the largest and therefore worst RMSE.

The influences of more atypical granulate material are examined in further experiments by integrating silicone granulate into the gripper type used for the membrane experiments in Fig. 24, as well as steel granulate in Figs. 25 and 26.

For the silicone granulate, all predictions appear to be skewed towards under-predicting the resulting gripping forces, with no particular advantage of any interpolation method. Averaged over all 31 objects, the experimental values for $C_{combined}$ surpassed the predicted values by over 60% for all approaches. The ANN-based method is only slightly more accurate compared to the linear models. Overall, the properties of the silicone granulate appear to increase the achievable gripping forces further within the adapted gripper design used for membrane

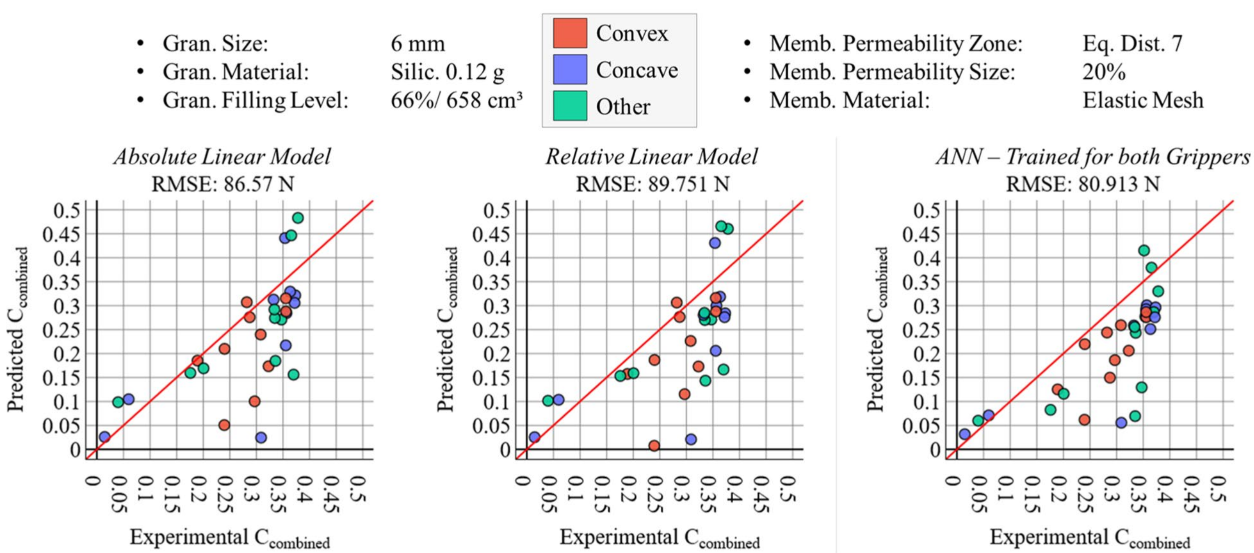

Fig. 24 Prediction of silicone granulate within a variation of the gripper type used for membrane variations, a perfect fit would be on the bisecting red line

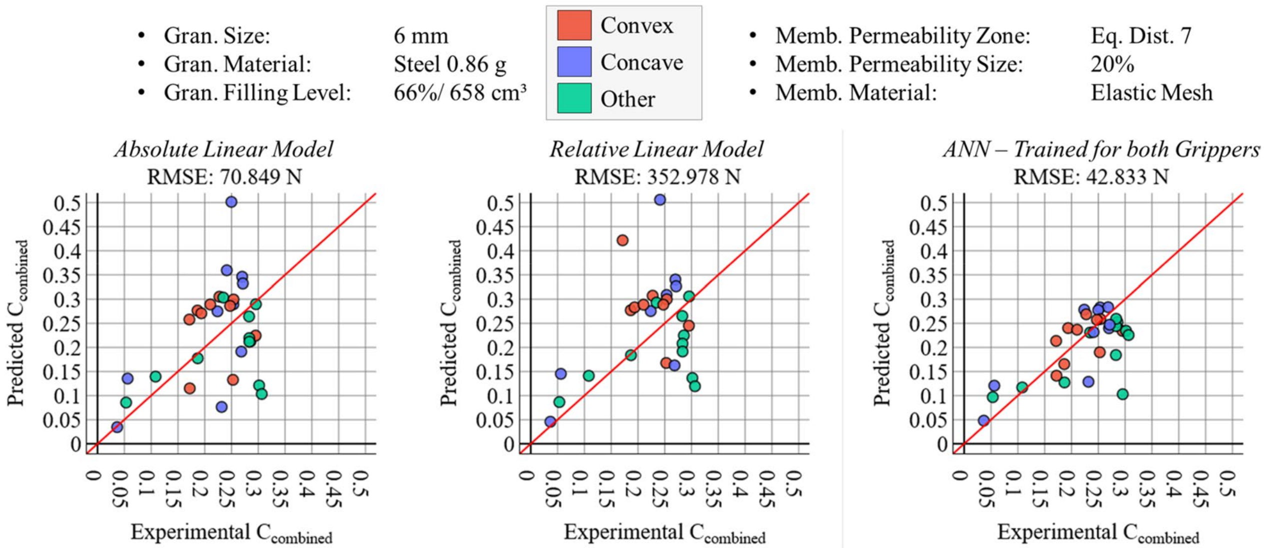

Fig. 25 Prediction of steel granulate within a variation of the gripper type used for membrane variations, a perfect fit would be on the bisecting red line

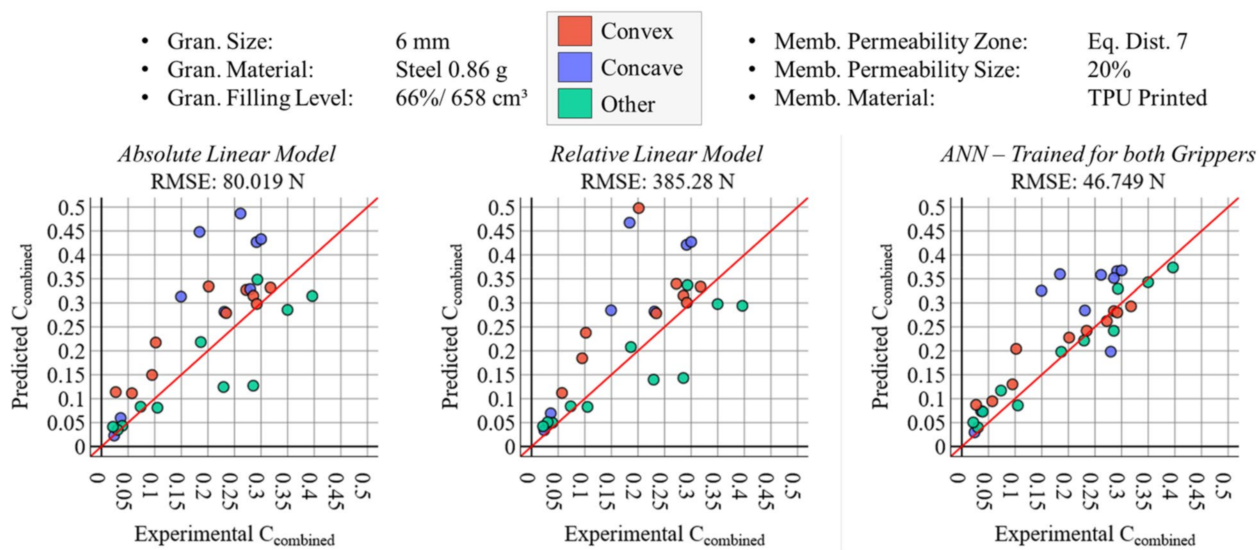

Fig. 26 Prediction of steel granulate within a variation of the gripper type with a TPU-based membrane, a perfect fit would be on the bisecting red line

variations. The currently proposed models are not able to properly assess the achievable gripping forces with the used input data and would have to be modified in order to enable an increased prediction quality.

Comparably higher accuracies appear to be possible with the steel granulate, as depicted in Figs. 25 and 26. Here, two experiments with equal settings for steel granulate are shown with the only difference being the membrane material.

For both experiments, the relative linear model results in very high values for the RMSE, as the model tends to amplify the predicted achievable gripping forces. For the relative linear models, the two tetrahedron geometries are not visible due to their unrealistic predictions of $C_{combined}$ exceeding 1.4, compared to the experimental value of 0.28. Here, the usage of steel granulate within the standard configuration for granular variations achieved an increase of the absolute value of 0.18, which corresponds to a relative increase of over 300% compared to the standard value. However, the base value for the standard configuration of the gripper used for membrane variations is already 0.348. Multiplied within the relative model, this leads to a large overestimation of the predicted value for $C_{combined}$. These findings underscore the different behavior of the two gripper designs and highlight the limits in comparability between the designs, particularly concerning this specific geometry. Without the three largest outliers, the RMSE of the relative linear model would shrink to 76.04 N, which is still slightly higher than the absolute linear model.

The absolute linear model therefore continues to establish itself as a more accurate prediction methodology in both configurations with steel granulate; however, it is still outperformed in accuracy by the ML-based methodology. Therefore, the ML-based approach remains the preferred and more accurate methodology for predicting achievable gripping forces.

Overall, the ANN-based prediction provided the consistently highest accuracies for all examined validation experiments (see Table 4), especially for ANNs trained to a specific gripper design. In spite of the differences between the capabilities of the different gripper types, an interpolation between gripper designs showed adequate results for a broad selection of configuration variations. Some outliers were interpolated especially with the relative linear model due to the nature of this approach. These outliers can be traced back to the differing base line in grippability for some more extreme shaped geometries between the two gripper types. For all examined experiments, the ANN-based approach exhibited superior accuracy; however, materials with additional effects on the gripping force, especially the silicone granulate, showed less predictable behavior compared to other tested parameters.

Future improvements, adjustments and adaptions

In general, all examined models would benefit from an increased quantity of data. Not only further experiments, although the presented approaches can already be described as extensive, but also simulations could be used for this. Especially a singled out examination of influences such as the elasticity of granulate material would be enabled with simulations. Empirical studies are restricted regarding the possibilities and availability of materials and therefore can often not merely assess the influence of a singular parameter, as it cannot rule out influences from unavoidably connected material properties such as material type, elasticity, surface roughness or weight being varied at the same time. Therefore, future investigations are highly advised to include simulative approaches in order to distinguish the influences from individual material properties further.

Additional influencing factors

To further expand the investigated influencing factors beyond the scope of this study, further variations could be included, such as the shape of the granulate material. By treating each factor as another individually evaluated independent factor, which was changed one at a time, an additional factor could therefore be implemented without a need for extensive repetitions of the over 10,000 experiments evaluated for this study.

Table 4 Overview of the results for the RMSE in Newton shown in Figs. 20, 21, 22, 23, 24, 25, 26 with the best predicted fit colored blue and underlined, worst fit in red

		Figure	Relative Linear Model	Absolute Linear Model	ANN for one Type of Gripper	ANN for both Types
Predicted within one Type of Gripper	Only Granular Variations	20	61.717	*Equal to relative linear model*	<u>31.454</u>	40.671
	Only Membrane Variations	21	54.611	*Equal to relative linear model*	<u>37.000</u>	51.550
Predicted for both Types of Gripper	Air-permeable Granulate, otherwise Standard	22	64.698	110.236	*N/A*	<u>59.541</u>
	Mixed Membrane and Granulate Variations	23	54.213	88.068	*N/A*	<u>48.024</u>
	Membrane Variations and Silicone Granulate	24	86.570	89.751	*N/A*	<u>80.913</u>
	Membrane Variations and Steel Granulate	25	70.849	352.978	*N/A*	<u>42.833</u>
	Other Membrane Variations and Steel Granulate	26	80.019	385.280	*N/A*	<u>46.749</u>

Prediction models

For the models without ML, standard Design of Experiments (DoE) -approaches could be applied, which would most likely require significant increases in the necessary experimental effort. A more complex non-linear model for the interactions is a possible result. However, this is suggested to require larger amounts of data for an accurate prediction compared to the ML-based approach, as this already exhibits an increased precision for all examined validation experiments. The ANN-based approach could be implemented as a model, which continuously increases the training data during the implementation, thereby improving the interpolation accuracy even for challenging materials such as the silicone granulate.

Selection and prediction methodology

To enhance the applicability of the presented methodology, it is essential to extend its capabilities beyond the limited set of geometries used in this study, which would merely enable predictions for the defined set of 31 geometries. A desirable future development would involve the ability to interpolate and predict $C_{combined}$ values for any arbitrary object surface. By establishing a connection between the presented interactions of the grippers regarding its configuration with the 31 examined objects and a methodology for arbitrary objects, a comprehensive framework for the applicability of the gripper would be achieved. This would enable a selection of an ideal gripper configuration for any geometry or partial surface area of a gripped object and would provide valuable insights for into a possible applicability within industrial handling processes. Therefore, an expansion towards an applicability for arbitrarily shaped geometries is necessary for an overall applicability of this methodology and should be a major goal for future expansions.

Conclusion

The goal of the presented research was the investigation of different configuration characteristics and their influences on the achievable gripping forces for a specific type of granular gripper and its modeling. Various influencing categories were defined, experimentally evaluated and analyzed in a one-factor-at-a-time setup. These factors were divided into granulate-based and membrane-based influences and examined using slightly adapted gripper types. As a result, the most influential parameters were found to be the granulate filling level, the membrane permeability as well as the membrane material. Notably, single granulate materials such as silicone and steel showed interesting effects, which could be examined more in the future. An approach for a prediction based on a statistical examination of the deviations over multiple experiments was presented. This framework allows for a selection of a suitable gripper configuration in accordance with process-specific requirements based on a presented spectrum of gripped objects.

To enable a prediction of achievable gripping forces over a full-factorial gripper configuration, prediction approaches of the experiments were examined. Absolute and relative linear models overarching different gripper designs were compared to an ML-based approach, particularly an ANN. Amongst these methods, the ANN-based approach achieved the highest accuracy for all seven exemplary examined validation experiments, followed by the absolute interpolation.

The key takeaways are summarized as follows:

- Achievable gripping forces can be predicted based on gripper configuration, and the deviation of the predicted achievable gripping force and therefore the certainty of a secure grip can also be approximated.
- Standard influencing parameters can be interpolated accurately within single designs of grippers, but face challenges when applied over different gripper designs.
- Approaches based on ML can be advantageous when transferring results of other types of grippers towards further developed designs.
- Configurations with more exotic materials, such as elastic silicone granulate, require additional attention and experiments due to their complex behavior.

Further adaptations are possible, but with the groundworks laid out within this research, a selection of influencing parameters can be gauged and predicted to provide a rough overview of achievable gripping forces for a wide spectrum of objects for implementations with the examined type of gripper.

Appendix

See Figs. 27, 28, 29, 30, 31 and 32.

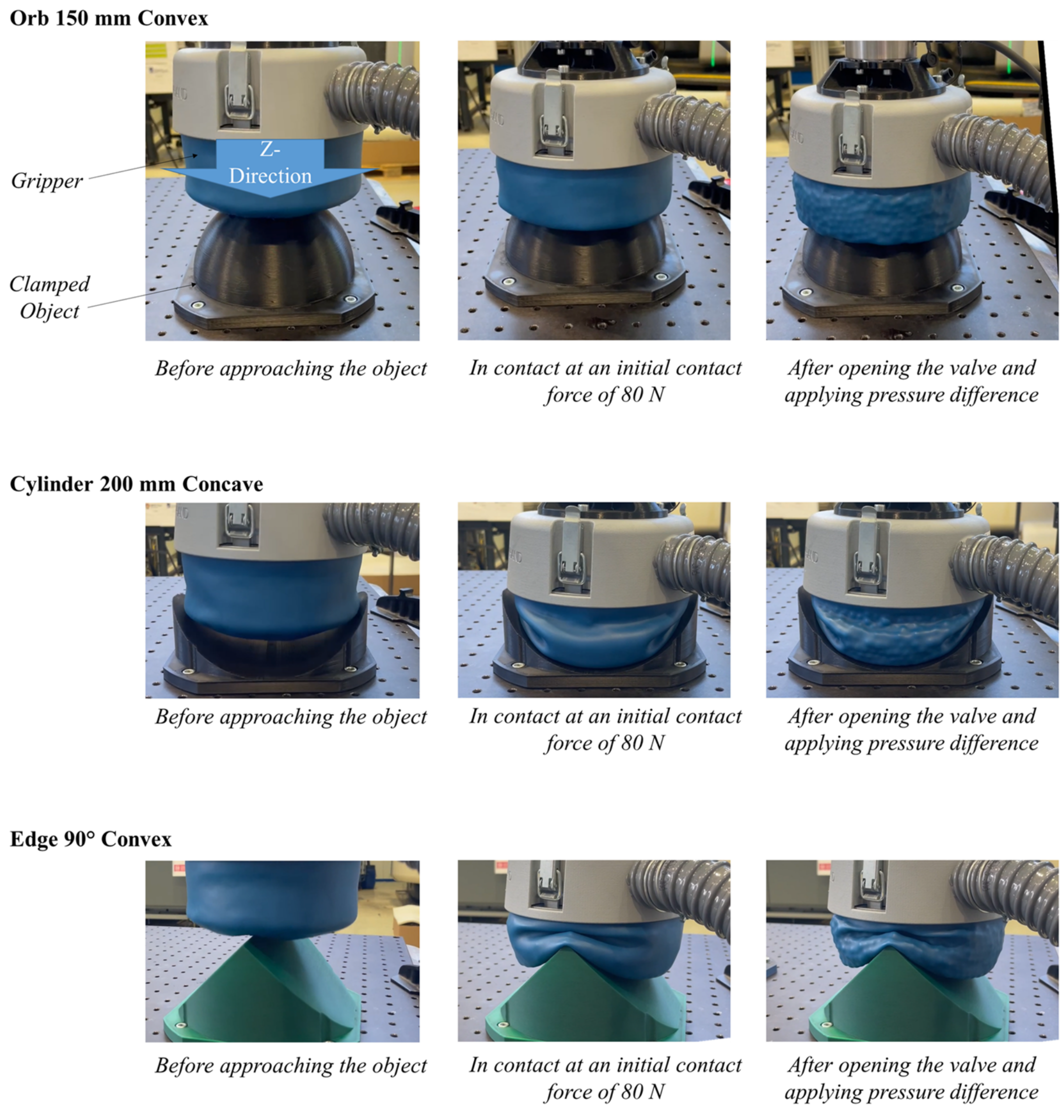

Fig. 27 Exemplary images of the standard configuration of the granulate variation gripper during the experiments for an excerpt of objects

Object name	Flat surface	Small flat surface ⌀100 mm	Small flat surface ⌀70 mm	Tetrahedron convex (90°)	Tetrahedron concave (90°)
Standard conf. for gran. variations $C_{combined}$	0.398	0.283	0.083	0.008	0.057
Standard conf. for memb. variations $C_{combined}$	0.367	0.203	0.050	0.232	0.348

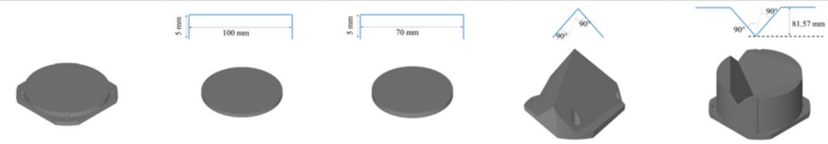

Corrugated surface 30 mm	Structured beads 30 mm/0%	Structured beads 30 mm/20%	Edged corrugated surface 30 mm	Corrugated surface 10 mm	Structured beads 10 mm/0%	Structured beads 10 mm/20%	Edged corrugated surface 10 mm
0.028	0.226	0.341	0.018	0.035	0.341	0.355	0.123
0.032	0.421	0.399	0.042	0.060	0.295	0.318	0.110

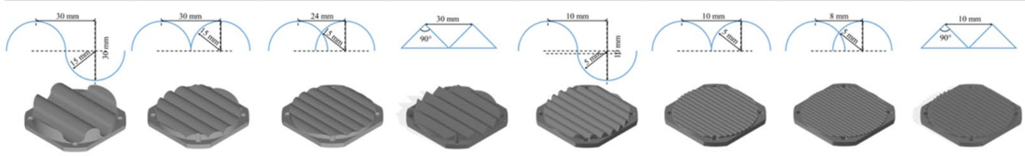

Cylinder ⌀200 mm convex	Cylinder ⌀200 mm concave	Cylinder ⌀150 mm convex	Cylinder ⌀150 mm concave	Cylinder ⌀100 mm convex	Cylinder ⌀100 mm concave
0.309	0.201	0.277	0.062	0.253	0.01
0.289	0.382	0.284	0.387	0.249	0.326

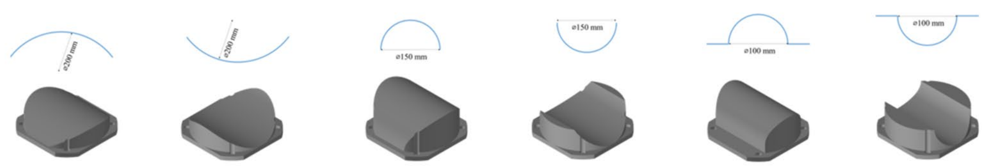

Edge 120° convex	Edge 120° concave	Edge 90° convex	Edge 90° concave	Edge 60° convex	Edge 60° concave
0.242	0.163	0.184	0.037	0.069	0.01
0.299	0.374	0.292	0.050	0.251	0.023

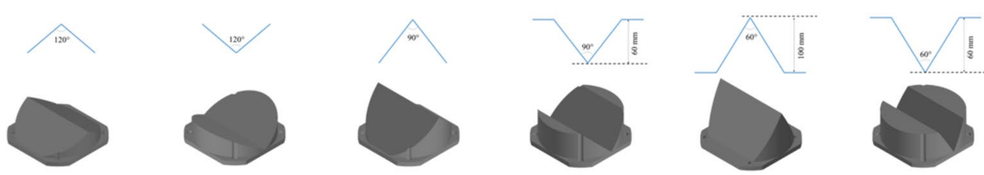

Orb ⌀200 mm convex	Orb ⌀200 mm concave	Orb ⌀150 mm convex	Orb ⌀150 mm concave	Orb ⌀100 mm convex	Orb ⌀100 mm concave
0.207	0.25	0.177	0.253	0.076	0.315
0.291	0.418	0.287	0.452	0.077	0.295

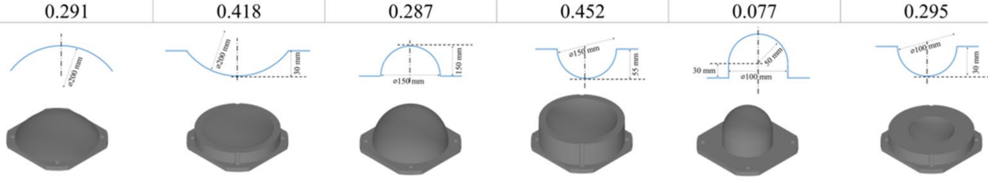

Fig. 28 Overview of resulting values for $C_{combined}$ for the 31 tested objects for the two standard configurations of the tested design variations, the stl files are available within the supplementary data

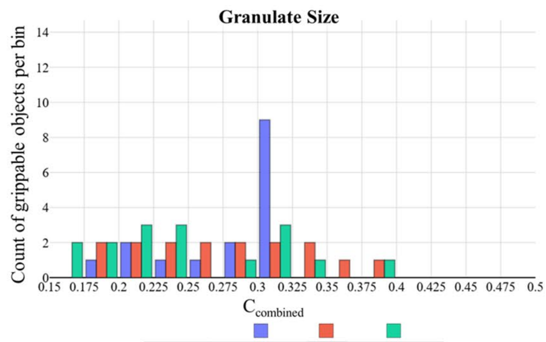

Feature	3 mm			6 mm	9 mm		
Δ to Standard	<-20%	<±20%	>20%	Standard	<-20%	<±20%	>20%
Convex	0	7	0	7	3	4	0
Concave	0	3	1	4	0	3	1
Other	1	4	0	5	0	5	0
Objects, where $C_{comb.}>0.15$	∑ 16 (=52%)			∑ 16 (=52%)	∑ 16 (=52%)		

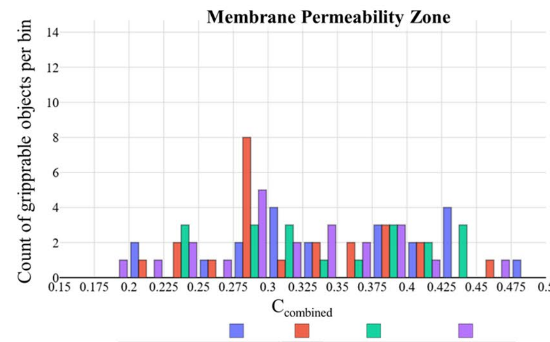

Feature	Equally Distributed 64			Equally Dist. 7	Middle			Outer Ring		
Δ to Standard	<-20%	<±20%	>20%	Standard	<-20%	<±20%	>20%	<-20%	<±20%	>20%
Convex	2	6	0	9	0	6	0	1	8	0
Concave	0	7	1	8	0	5	2	1	7	0
Other	0	5	0	6	0	6	0	0	5	0
Objects, where $C_{comb.}>0.15$	∑ 21 (=68%)			∑ 23 (=75%)	∑ 19 (=61%)			∑ 22 (=71%)		

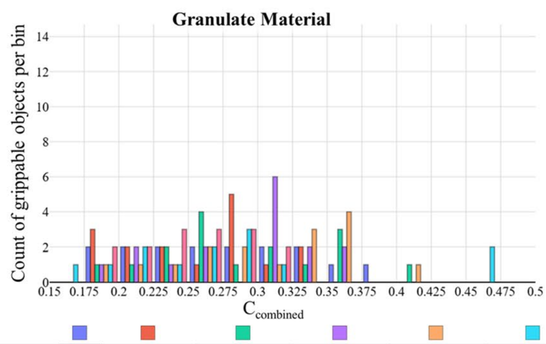

Feature	ABS 0.12 g	ABS 0.20 g			Brass hl. 0.16 g			PET hl. 0.12 g			PET 0.12 g			Silicone 0.12 g			Steel 0.86 g		
Δ to Standard	Standard	<-20%	<±20%	>20%	<-20%	<±20%	>20%	<-20%	<±20%	>20%	<-20%	<±20%	>20%	<-20%	<±20%	>20%	<-20%	<±20%	>20%
Convex	7	0	7	0	0	5	2	0	4	3	0	7	0	1	5	0	0	5	2
Concave	4	0	4	0	0	3	1	0	4	0	0	2	2	0	3	1	0	4	0
Other	5	1	4	0	0	5	0	0	5	0	0	5	0	1	1	3	3	1	0
Objects, where $C_{comb.}>0.15$	∑ 16	∑ 16 (=52%)			∑ 16 (=52%)			∑ 16 (=52%)			∑ 16 (=52%)			∑ 15 (=48%)			∑ 15 (=48%)		

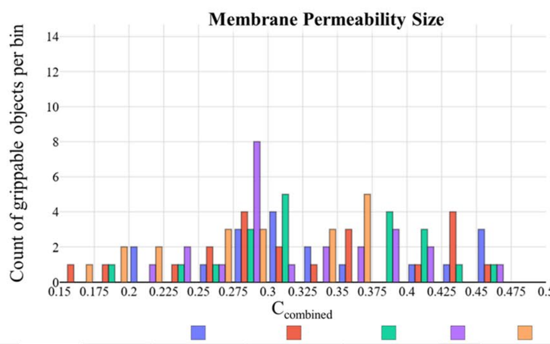

Feature	5%			20%			35%			50%	65%		
Δ to Standard	<-20%	<±20%	>20%	<-20%	<±20%	>20%	<-20%	<±20%	>20%	Standard	<-20%	<±20%	>20%
Convex	0	5	0	1	6	0	0	6	0	9	3	4	0
Concave	2	5	1	0	8	0	0	7	1	8	1	6	0
Other	2	3	0	0	5	1	0	6	0	6	1	4	0
Objects, where $C_{comb.}>0.15$	∑ 18 (=58%)			∑ 21 (=68%)			∑ 20 (=65%)			∑ 23 (=74%)	∑ 19 (=61%)		

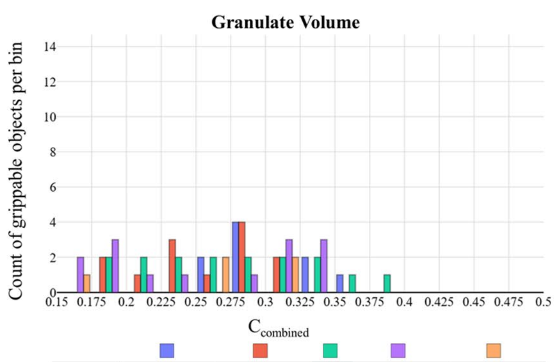

Feature	33%/ 329 ml			50%/ 493 ml			66%/ 658 ml	83.3%/ 822 ml			100%/ 986 ml		
Δ to Standard	<-20%	<±20%	>20%	<-20%	<±20%	>20%	Standard	<-20%	<±20%	>20%	<-20%	<±20%	>20%
Convex	0	3	2	0	6	1	7	3	2	0	1	0	0
Concave	0	1	0	0	3	0	4	0	3	1	0	2	1
Other	2	1	0	2	1	0	5	1	4	0	0	1	0
Objects, where $C_{comb.}>0.15$	∑ 9 (=29%)			∑ 13 (=42%)			∑ 16 (=52%)	∑ 14 (=45%)			∑ 5 (=16%)		

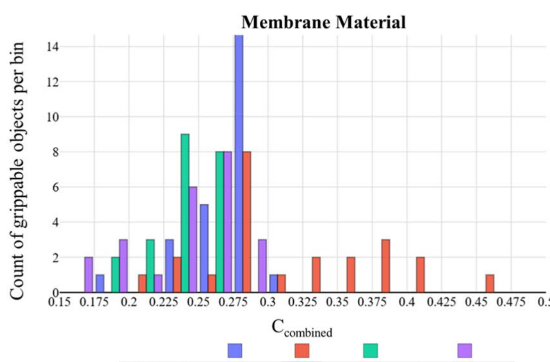

Feature	Elastic Mesh			TPU Printed	Nylon 70den			Nylon 40den		
Δ to Standard	<-20%	<±20%	>20%	Standard	<-20%	<±20%	>20%	<-20%	<±20%	>20%
Convex	1	8	1	9	4	3	1	4	3	1
Concave	5	2	0	8	7	1	0	7	0	0
Other	2	3	3	6	4	1	1	3	2	3
Objects, where $C_{comb.}>0.15$	∑ 25 (=81%)			∑ 23 (=74%)	∑ 22 (=71%)			∑ 23 (=75%)		

Fig. 29 Overview of the results for the variation of granulate size with a focus on objects surpassing a value for $C_{combined}$ of 0.15

Gripper Type	Standard Granular Gripper	Standard Granular Gripper	Standard Granular Gripper	**Standard Granular Gripper**	Standard Granular Gripper	Standard Granular Gripper	Standard Granular Gripper	Standard Granular Gripper	Standard Granular Gripper	Standard Granular Gripper	Standard Granular Gripper	Standard Granular Gripper	Standard Granular Gripper
Granulate Size	3 mm	6 mm	6 mm	**6 mm**	6 mm	6 mm	9 mm	6 mm	6 mm	6 mm	6 mm	6 mm	6 mm
Granulate Material	ABS 0.12 g	ABS 0.12 g	ABS 0.12 g	**ABS 0.12 g**	ABS 0.12 g	ABS 0.12 g	ABS 0.12 g	ABS 0.20 g	Brass 0.16 g hl.	PET 0.12 g hl.	PET 0.12 g	Silicone 0.12 g	Steel 0.86 g
Granulate Filling Level	658 cm³	329 cm³	493 cm³	**658 cm³**	822 cm³	986 cm³	658 cm³	658 cm³	658 cm³	658 cm³	658 cm³	658 cm³	658 cm³
Arrangement of Membrane Permeability Zone	Standard Granular Gripper	Standard Granular Gripper	Standard Granular Gripper	**Standard Granular Gripper**	Standard Granular Gripper	Standard Granular Gripper	Standard Granular Gripper	Standard Granular Gripper	Standard Granular Gripper	Standard Granular Gripper	Standard Granular Gripper	Standard Granular Gripper	Standard Granular Gripper
Size of Membrane Permeability	Standard Granular Gripper	Standard Granular Gripper	Standard Granular Gripper	**Standard Granular Gripper**	Standard Granular Gripper	Standard Granular Gripper	Standard Granular Gripper	Standard Granular Gripper	Standard Granular Gripper	Standard Granular Gripper	Standard Granular Gripper	Standard Granular Gripper	Standard Granular Gripper
Membrane Material	Standard Granular Gripper	Standard Granular Gripper	Standard Granular Gripper	**Standard Granular Gripper**	Standard Granular Gripper	Standard Granular Gripper	Standard Granular Gripper	Standard Granular Gripper	Standard Granular Gripper	Standard Granular Gripper	Standard Granular Gripper	Standard Granular Gripper	Standard Granular Gripper
Flat surface	-20.9%	-29.9%	-41.7%	*Standard*	-40.4%	BT -63.3 %	-4.7%	-26.9%	-9.2%	4.8%	-9.4%	69.8%	-39.4%
Small flat surface 100 mm	7.7%	1.2%	0.2%	*Standard*	9.6%	-3.3%	-14.8%	3.9%	13.6%	19.4%	6.9%	9.1%	13.2%
Small flat surface 70 mm	BT 15.5 %	BT -11.3 %	BT -2.9 %	BT Standard	BT -4.4 %	BT -17.2 %	BT -8.9 %	BT 3.7 %	BT 1.9 %	BT 19.9 %	BT -0.6 %	BT 30.9 %	BT -5.1 %
Tetrahedron convex (90°)	BT -45.0 %	BT 305.3 %	BT 48.8 %	BT Standard	BT -42.5 %	BT 23.8 %	BT -42.0 %	BT 119.4 %	BT -22.8 %	BT 64.4 %	BT -23.2 %	BT -19.3 %	BT 831.1 %
Tetrahedon concave (90°)	BT -15.3 %	BT -84.4 %	BT -53.9 %	BT Standard	BT 29.3 %	BT 34.8 %	BT 48.5 %	BT 23.4 %	BT 59.5 %	BT -18.8 %	BT 114.5 %	BT -11.0 %	BT 323.4 %
Corr. surface 30 mm	BT -2.4 %	BT -68.9 %	BT -22.1 %	BT Standard	BT -7.7 %	BT 25.0 %	BT -45.8 %	BT 56.0 %	BT -5.5 %	BT -18.2 %	BT 23.7 %	BT 69.3 %	BT 22.7 %
Structured beads 30 mm/0%	BT -36.6 %	BT -49.2 %	BT -34.6 %	BT Standard	BT -42.0 %	BT -63.4 %	BT -15.2 %	BT -17.9 %	BT -5.5 %	BT -1.0 %	BT -4.1 %	BT -21.2 %	BT -5.9 %
Structured beads 30 mm/20%	-11.7%	BT -41.5 %	BT -27.7 %	*Standard*	-3.8%	BT -56.2 %	-10.3%	-4.2%	-5.9%	2.9%	-7.6%	33.3%	BT -35.5 %
Edged corr. surface 30 mm	BT -27.2 %	BT -20.2 %	BT 20.3 %	BT Standard	BT 4.3 %	BT 100.6 %	BT -6.3 %	BT 16.0 %	BT 54.7 %	BT 37.1 %	BT 10.9 %	BT -17.3 %	BT 67.0 %
Corr. surface 10 mm	BT -29.8 %	BT -80.0 %	BT -26.3 %	BT Standard	BT -30.6 %	BT 16.1 %	BT -0.4 %	BT -7.3 %	BT 14.0 %	BT -17.2 %	BT -17.1 %	BT -25.2 %	BT 25.7 %
Structured beads 10 mm/0%	-12.0%	BT -37.7 %	BT -39.7 %	*Standard*	-5.6%	BT -43.4 %	-7.3%	-4.0%	5.7%	9.0%	-1.5%	-22.8%	-33.0%
Structured beads 10 mm/20%	-14.8%	-27.6%	-35.6%	*Standard*	-5.6%	BT -58.6 %	-1.7%	-18.9%	12.8%	3.3%	1.9%	62.7%	-44.4%
Edged corr. surface 10 mm	BT -11.9 %	BT -42.5 %	BT -22.4 %	BT Standard	BT -22.0 %	BT -10.2 %	BT -8.7 %	BT 0.3 %	BT 14.1 %	BT 17.2 %	BT 4.4 %	BT -1.6 %	BT -7.0 %
Cylinder 200 mm convex	4.5%	12.5%	1.0%	*Standard*	-28.9%	-48.5%	-25.4%	-8.1%	6.3%	10.2%	3.9%	-3.8%	-13.2%
Cylinder 200 mm concave	3.2%	BT -68.9 %	BT -8.1 %	*Standard*	-15.1%	BT -44.9 %	0.7%	-2.7%	20.5%	16.6%	-3.4%	-16.4%	-3.2%
Cylinder 150 mm convex	13.8%	26.2%	13.7%	*Standard*	-33.4%	BT -50.6 %	-21.8%	1.3%	6.3%	18.2%	10.0%	1.3%	5.4%
Cylinder 150 mm concave	BT 130.7 %	BT 11.8 %	BT -12.6 %	BT Standard	BT 124.1 %	BT 23.9 %	BT 120.0 %	BT 71.9 %	BT 153.5 %	BT -1.1 %	BT 22.9 %	BT -3.3 %	BT 45.2 %
Cylinder 100 mm convex	13.2%	17.8%	11.6%	*Standard*	-33.5%	BT -69.4 %	-24.7%	-4.3%	2.6%	24.6%	8.4%	18.3%	11.2%
Cylinder 100 mm concave	BT -51.7 %	BT -31.8 %	BT 27.0 %	BT Standard	BT 5.2 %	BT 57.6 %	BT -48.7 %	BT 35.1 %	BT -66.2 %	BT 9.0 %	BT -47.0 %	BT -1.1 %	BT 501.6 %
Edge 120° convex	3.8%	10.6%	9.0%	*Standard*	-18.8%	BT -59.6 %	-16.3%	0.7%	7.3%	11.1%	7.0%	-23.5%	3.6%
Edge 120° concave	BT -39.6 %	BT -30.4 %	BT 14.9 %	BT Standard	BT -46.3 %	BT -75.9 %	BT -5.9 %	BT -4.9 %	BT -1.0 %	BT 8.3 %	BT -14.4 %	BT -17.7 %	BT -2.7 %
Edge 90° convex	4.6%	BT -38.8 %	7.6%	*Standard*	BT -43.5 %	BT -86.0 %	-13.7%	5.5%	6.0%	7.3%	9.4%	BT -21.5 %	11.5%
Edge 90° concave	BT -41.4 %	BT -75.8 %	BT -17.4 %	BT Standard	BT -72.2 %	BT -77.9 %	BT -11.6 %	BT 63.5 %	BT -48.4 %	BT 31.1 %	BT -28.6 %	BT -8.6 %	BT 75.1 %
Edge 60° convex	BT -15.3 %	BT -56.6 %	BT -64.0 %	BT Standard	BT -84.7 %	BT -78.6 %	BT -42.8 %	BT 31.6 %	BT -33.4 %	BT -44.4 %	BT 5.3 %	BT -15.2 %	BT 89.7 %
Edge 60° concave	BT -7.0 %	BT -22.5 %	BT -22.4 %	BT Standard	BT 36.2 %	BT 195.7 %	BT 16.5 %	BT 23.7 %	BT -9.4 %	BT -20.9 %	BT 9.1 %	BT -3.7 %	BT 86.1 %
Orb 200 mm convex	14.9%	68.4%	42.3%	*Standard*	-8.3%	BT -43.7 %	-7.8%	7.8%	22.1%	38.3%	9.3%	-0.6%	24.1%
Orb 200 mm concave	24.0%	BT -62.0 %	-7.4%	*Standard*	16.0%	5.6%	-2.8%	1.5%	8.3%	18.0%	28.3%	-6.7%	-17.0%
Orb 150 mm convex	12.9%	BT -29.1 %	1.1%	*Standard*	BT -17.9 %	BT -47.6 %	-8.0%	5.6%	31.7%	21.6%	13.7%	13.6%	31.9%
Orb 150 mm concave	16.4%	BT -44.5 %	-15.0%	*Standard*	35.3%	23.2%	20.3%	-13.0%	-13.0%	6.7%	28.7%	7.7%	9.7%
Orb 100 mm convex	BT 1.3 %	BT -65.0 %	BT -32.5 %	BT Standard	BT -59.8 %	BT -46.1 %	BT -32.2 %	BT 9.8 %	BT 51.5 %	BT 53.4 %	BT -0.3 %	BT 77.7 %	BT 78.7 %
Orb 100 mm concave	-0.7%	-12.0%	-6.9%	*Standard*	-2.8%	0.7%	-8.5%	2.1%	16.1%	16.6%	2.9%	50.4%	-2.4%

BT Below grippability threshold of $C_{combined} = 0.15$ or under 100 N for all experiments and therefore excluded

Increase of over 20% compared to the respective standard configuration

Decrease of over 20% compared to the respective standard configuration

Fig. 30 Overview of the resulting relative differences for $C_{combined}$ for varied granulate parameters in relation to its standard configuration in percent

Gripper Type	Standard Membrane Gripper	Standard Membrane Gripper	Standard Membrane Gripper	Standard Membrane Gripper	Standard Membrane Gripper	**Standard Membrane Gripper**	Standard Membrane Gripper	Standard Membrane Gripper	Standard Membrane Gripper	Standard Membrane Gripper	Standard Membrane Gripper
Granulate Size	6 mm	6 mm	6 mm	6 mm	6 mm	**6 mm**	6 mm	6 mm	6 mm	6 mm	6 mm
Granulate Material	ABS 0.12 g	ABS 0.12 g	ABS 0.12 g	ABS 0.12 g	ABS 0.12 g	**ABS 0.12 g**	ABS 0.12 g	ABS 0.12 g	ABS 0.12 g	ABS 0.12 g	ABS 0.12 g
Granulate Filling Level	$658\ cm^3$	$658\ cm^3$	$658\ cm^3$	$658\ cm^3$	$658\ cm^3$	**$658\ cm^3$**	$658\ cm^3$	$658\ cm^3$	$658\ cm^3$	$658\ cm^3$	$658\ cm^3$
Arrangement of Membrane Permeability Zone	Equally Dist. 64	Equally Dist. 7	Equally Dist. 7	Equally Dist. 7	Equally Dist. 7	**Equally Dist. 7**	Equally Dist. 7	Equally Dist. 7	Equally Dist. 7	Middle	Outer Ring
Size of Membrane Permeability	50%	5%	20%	35%	50%	**50%**	50%	50%	65%	50%	50%
Membrane Material	TPU Printed	TPU Printed	TPU Printed	TPU Printed	Elastic Mesh	**TPU Printed**	Nylon 70den	Nylon 40den	TPU Printed	TPU Printed	TPU Printed
Flat surface	6.7%	-5.0%	20.4%	5.9%	-19.9%	*Standard*	-26.9%	-24.8%	-0.1%	6.3%	11.7%
Small flat surface 100 mm	*BT -35.1 %*	*BT -32.6 %*	-10.9%	-2.4%	41.9%	*Standard*	29.1%	45.5%	0.3%	13.4%	*BT 3.4 %*
Small flat surface 70 mm	*BT -64.8 %*	*BT 47.8 %*	*BT 71.2 %*	*BT 48.4 %*	*BT 117.0 %*	*BT Standard*	*BT 192.4 %*	*BT 238.9 %*	*BT 6.8 %*	*BT 118.1 %*	*BT -42.4 %*
Tetrahedron convex (90°)	*BT -96.7 %*	*BT -97.2 %*	*BT -78.0 %*	*BT -95.5 %*	0.5%	*Standard*	*BT -20.8 %*	*BT -27.4 %*	*BT -72.5 %*	*BT -90.8 %*	-16.3%
Tetrahedon concave (90°)	11.8%	4.1%	5.1%	-7.2%	-13.6%	*Standard*	-25.5%	-27.0%	4.2%	24.7%	8.6%
Corr. surface 30 mm	*BT -41.8 %*	*BT -73.6 %*	*BT 9.4 %*	*BT 31.6 %*	*BT 138.9 %*	*BT Standard*	*BT 155.8 %*	*BT 286.7 %*	*BT -1.8 %*	*BT 11.4 %*	*BT -22.3 %*
Structured beads 30 mm/0%	0.4%	-29.5%	-14.2%	-3.4%	-30.6%	*Standard*	-38.4%	-34.0%	*BT -37.2 %*	-1.7%	-8.0%
Structured beads 30 mm/20%	6.8%	10.1%	9.2%	-3.9%	-25.7%	*Standard*	-36.4%	-35.3%	-17.9%	7.3%	-12.8%
Edged corr. surface 30 mm	*BT -31.0 %*	*BT -82.8 %*	*BT -46.9 %*	*BT -19.0 %*	601.3%	*BT Standard*	*BT 457.7 %*	532.8%	*BT -17.1 %*	*BT 3.9 %*	*BT -16.2 %*
Corr. surface 10 mm	*BT -9.1 %*	*BT -82.5 %*	*BT -42.8 %*	*BT -5.6 %*	*BT 223.8 %*	*BT Standard*	*BT 123.0 %*	*BT 133.5 %*	*BT -15.7 %*	*BT -5.3 %*	*BT 14.7 %*
Structured beads 10 mm/0%	-4.7%	-24.2%	-19.6%	-6.5%	-1.1%	*Standard*	-21.1%	-12.0%	-23.9%	-4.3%	-1.2%
Structured beads 10 mm/20%	2.3%	-5.5%	-10.7%	-2.5%	-7.5%	*Standard*	-17.6%	-17.0%	-12.5%	-4.9%	-4.4%
Edged corr. surface 10 mm	*BT 7.5 %*	*BT -73.7 %*	*BT -16.4 %*	*BT 3.8 %*	165.3%	*BT Standard*	*BT 64.6 %*	108.1%	*BT 0.0 %*	*BT 0.1 %*	*BT 9.2 %*
Cylinder 200 mm convex	18.9%	10.0%	17.2%	5.6%	-4.1%	*Standard*	-21.1%	-34.4%	-5.9%	-2.1%	3.8%
Cylinder 200 mm concave	15.8%	19.6%	14.9%	7.9%	-26.3%	*Standard*	-37.2%	-54.9%	-2.6%	11.3%	1.7%
Cylinder 150 mm convex	11.8%	-6.4%	5.2%	10.8%	-5.4%	*Standard*	-21.1%	-29.7%	-9.5%	12.8%	2.3%
Cylinder 150 mm concave	10.8%	18.9%	18.5%	6.8%	-32.9%	*Standard*	-38.5%	-59.7%	-6.6%	7.3%	-4.8%
Cylinder 100 mm convex	17.8%	*BT -60.4 %*	0.9%	3.4%	4.1%	*Standard*	-10.2%	-19.8%	-26.5%	-2.6%	13.1%
Cylinder 100 mm concave	37.4%	40.3%	-15.0%	34.6%	*BT -77.4 %*	*Standard*	-18.1%	*BT -68.3 %*	*BT -91.4 %*	*BT -88.4 %*	12.3%
Edge 120° convex	8.0%	6.9%	8.2%	4.4%	-8.9%	*Standard*	-24.1%	-23.4%	-0.7%	3.4%	-0.6%
Edge 120° concave	10.1%	9.5%	15.1%	0.4%	-21.5%	*Standard*	-47.3%	-38.1%	-9.7%	6.2%	-7.0%
Edge 90° convex	5.8%	-3.6%	4.6%	-0.6%	-19.3%	*Standard*	-32.0%	-35.5%	-4.6%	1.0%	-14.0%
Edge 90° concave	*BT -16.9 %*	*BT -77.2 %*	*BT -35.7 %*	*BT -21.9 %*	*BT 152.3 %*	*BT Standard*	*BT 224.5 %*	*BT 128.9 %*	*BT -10.7 %*	*BT -21.1 %*	*BT 8.1 %*
Edge 60° convex	7.6%	-16.8%	8.1%	-2.6%	-30.3%	*Standard*	*BT -37.0 %*	*BT -41.8 %*	-25.3%	-1.5%	-19.9%
Edge 60° concave	*BT -18.6 %*	*BT -80.5 %*	*BT -36.2 %*	*BT -3.7 %*	*BT 51.7 %*	*BT Standard*	*BT -17.6 %*	*BT 21.9 %*	*BT -42.0 %*	*BT 5.7 %*	*BT 3.6 %*
Orb 200 mm convex	-30.5%	*BT -83.4 %*	-42.6%	*BT -51.8 %*	2.5%	*Standard*	-19.6%	-9.7%	-47.4%	*BT -49.9 %*	-17.5%
Orb 200 mm concave	-4.3%	-26.8%	-14.9%	-10.2%	-29.2%	*Standard*	-44.4%	-44.2%	-34.6%	-18.5%	-22.6%
Orb 150 mm convex	-28.7%	*BT -89.0 %*	*BT -67.6 %*	*BT -61.1 %*	-5.8%	*Standard*	-17.0%	-5.4%	*BT -59.3 %*	*BT -55.7 %*	-20.9%
Orb 150 mm concave	6.9%	-28.1%	-6.4%	0.0%	-35.1%	*Standard*	-42.6%	-44.1%	-18.8%	-13.8%	3.0%
Orb 100 mm convex	*BT -80.5 %*	*BT -74.2 %*	*BT -32.6 %*	*BT -18.0 %*	215.6%	*BT Standard*	177.0%	202.7%	*BT -27.4 %*	*BT 63.0 %*	*BT -46.8 %*
Orb 100 mm concave	5.5%	-1.9%	-1.8%	-4.1%	-2.3%	*Standard*	-23.3%	-22.1%	15.4%	23.2%	14.7%

BT Below grippability threshold of $C_{combined} = 0.15$ or under 100 N for all experiments and therefore excluded

Increase of over 20% compared to the respective standard configuration

Decrease of over 20% compared to the respective standard configuration

Fig. 31 Overview of the resulting relative differences for $C_{combined}$ for varied membrane parameters in relation to its standard configuration in percent

Granulate	Weight of 250 cm³ in g	Median of 3 funnel passing times for 250 cm³ in s	Avg. resulting strain for a 150 N load on 250 cm³ granulate within a cylinder with a diameter of 35 mm (3 samples)
ABS 3 mm	145.31	03:46	0.55%
ABS 6 mm 0.12 g	158.51	03:59	0.44%
ABS 9 mm	131.72	10:16	0.71%
ABS 0.20 g	286.30	04:09	0.43%
Brass hollow 0.16 g	230.81	05:41	0.77%
PET hl. 0.12 g	94.26	06:37	0.99%
PET 0.12 g	161.07	05:46	0.85%
Silicone 0.12 g	158.10	09:37	15.99%
Steel 6 mm 0.86 g	1230.49	04:42	0.49%
Steel 3 mm 0.11 g (used for validation)	1271.09	03:46	0.32%

Membrane	g/m²	Avg. adhesive coefficient of friction for 0.0075 N/mm² (from three tests for 100x200 mm samples with a 10x10 mm PLA partner - R_a = 1.13; R_z = 5.88; R_{max} = 7.12 - measured on an inclined plane, definition breakaway as a speed of 0.5 mm/s)	Avg. resulting strain % for 50 N (from three tensile tests for samples with the clamped base length of 200 mm and a width of 50 mm)
Elastic Mesh	508.69	1.665	104.51%
TPU Printed	652.17	0.704	10.39%
Nylon 70den	166.34	0.659	3.03%
Nylon 40den	69.56	0.492	5.59%
Standard TPU for the granular gripper	2811.30	1.243	17.36%

Fig. 32 Overview over quantifying parameters for the examined materials, further information for the experimental procedures can be found within the supplementary material, granulate experiments were performed in accordance with [14]

Acknowledgements
We acknowledge support by the German Research Foundation and the Open Access Publication Funds of Technische Universität Braunschweig.

Author contributions
Conceptualization: C.W. and N.D.; methodology: C.W.; software: C.W.; validation: C.W. and N.D.; formal analysis: C.W. and N.D.; investigation: C.W. and N.D.; resources: A.K. and K.D.; data curation: C.W.; writing—original draft preparation: C.W., N.D.; writing—review and editing: A.K. and K.D.; visualization: C.W.; supervision: A.K. and K.D.; project administration: A.K. and K.D.; funding acquisition: A.K. and K.D. All authors have read and agreed to the published version of the manuscript.

Funding
Open Access funding enabled and organized by Projekt DEAL. The support of the German National Science Foundation (Deutsche Forschungsgemeinschaft DFG) through the funding of the research project 'ModPro' (450839725) is gratefully acknowledged.

Availability of data and materials
Data supporting the reported results, including code and graphs, can be found at the following link: https://lnk.tu-bs.de/7ojE8i (Accessed on 12.12.2023).

Declarations

Ethics approval and consent to participate
Not applicable.

Consent for publication
Not applicable.

Competing interests
The authors declare no conflict of interest or competing interests.

Received: 4 August 2023 Accepted: 16 December 2023
Published online: 05 January 2024

References

1. Birglen L, Schlicht T (2018) A statistical review of industrial robotic grippers. Robot Comp Integr Manuf 49:88
2. Pham D, Yeo S (1991) Strategies for gripper design and selection in robotic assembly. Int J Prod Res 29:303–16
3. Gabriel F, Römer M, Bobka P et al (2021) Model-based grasp planning for energy-efficient vacuum-based handling. CIRP Annals 70(1):1–4
4. Kehoe B, Berenson D, Goldberg K (2012) Estimating part tolerance bounds based on adaptive Cloud-based grasp planning with slip. In: IEEE International Conference, pp 1106–1113
5. Navarro-Guerrero N, Toprak S, Josifovski J, Jamone L (2023) Visuo-haptic object perception for robots: an overview. Auton Robots. 47(4):377–403
6. Azim MS, Lobov A, Pastukhov A (2019) Methodology for implementing universal gripping solution for robot application. Proc Estonian Acad Sci 68:4
7. Shintake J, Cacucciolo V, Floreano D et al (2018) Soft robotic grippers. Adv Mater. 30(29):1707035
8. Mykhailyshyn R, Savkiv V, Maruschak P et al (2022) A systematic review on pneumatic gripping devices for industrial robotics. Transport 37(3):201–31
9. Götz H, Santarossa A, Sack A et al (2022) Soft particles reinforce robotic grippers: robotic grippers based on granular jamming of soft particles. Granular Matter 24:1
10. Fitzgerald SG, Delaney GW, Howard D (2020) A review of jamming actuation in soft robotics. Actuators 9:1
11. Brown E, Rodenberg N, Amend J et al (2010) Universal robotic gripper based on the jamming of granular material. Proc Natl Acad Sci USA 107(44):18809–14
12. Santarossa A, D'Angelo O, Sack A, Pöschel T (2023) Effect of particle size on the suction mechanism in granular grippers. Granular Matter. 25(1):16
13. Dröder K, Dietrich F, Löchte C et al (2016) Model based design of process-specific handling tools for workpieces with many variants in shape and material. CIRP Annals 65(1):53–6
14. Löchte CW (2016) Formvariable Handhabung mittels granulatbasierter Niederdruckflächensauger. Dissertation, TU Braunschweig
15. Kunz H, Löchte C, Dietrich F, Raatz A, Fischer F, Dröder K, Dilger K (2015) Novel form-flexible handling and joining tool for automated preforming. Sci Eng Comp Mater 22(2):199–213
16. Wacker C, Dierks N, Illgen J et al. (2022) Empirically Adapted Model for the Handling of Variable Geometries with Vacuum-Based Granulate Grippers. Proceedings of the 7th MHI Colloquium 2022

17. Nishida T, Shigehisa D, Kawashima N et al. (2014) Development of universal jamming gripper with a force feedback mechanism. In: 2014 Joint 7th International Conference on Soft Computing and Intelligent Systems (SCIS) and 15th International Symposium on Advanced Intelligent Systems (ISIS), pp 242–246
18. Shanmugasundar G, Dharanidharan M, Vishwa D et al. (2022) A study on design of universal gripper for different part handling: Methods, mechanisms, and materials. In: RECENT TRENDS IN SCIENCE AND ENGINEERING, p 20115
19. Friedmann M, Fleischer J (2022) Automated configuration of modular gripper fingers. Procedia CIRP 106:70–75
20. Mishra R, Philips T, Delaney GW et al. (2021) Vibration Improves Performance in Granular Jamming Grippers
21. Schmalz J (2018) Rechnergestützte Auslegung und Auswahl von Greifersystemen. Dissertation, TU München
22. Amend JR, Brown E, Rodenberg N et al (2012) A positive pressure universal gripper based on the jamming of granular material. IEEE Trans Robot 28(2):341–50
23. Amend J, Cheng N, Fakhouri S et al (2016) Soft robotics commercialization: jamming grippers from research to product. Soft Robot 3(4):213–22
24. Meuleman S, Balt V, Jarray A et al. (2017) Investigation of Particle Properties on the Holding Force in a Granular Gripper. V International Conference on Particle-based Methods - Fundamentals and Applications
25. Alsakarneh A, Alnaqbi S, Alkaabi M et al. (2018) Experimental analysis of the holding-force of the jamming grippers. In: 2018 Advances in Science and Engineering Technology International Conferences (ASET), pp 1–3
26. Fujita M, Tadakuma K, Komatsu H et al (2018) Jamming layered membrane gripper mechanism for grasping differently shaped-objects without excessive pushing force for search and rescue missions. Adv Robot 32(11):590–604
27. Miettinen J, Frilund P, Vuorinen I et al (2019) Granular jamming based robotic gripper for heavy objects. Proc Estonian Acad Sci 68(4):421–8
28. Howard D, O'Connor J, Brett J et al. (2021) Shape, Size, and Fabrication Effects in 3D Printed Granular Jamming Grippers. In: 2021 IEEE 4th International Conference on Soft Robotics (RoboSoft), pp 458–464
29. Gómez-Paccapelo JM, Santarossa AA, Bustos HD et al (2021) Effect of the granular material on the maximum holding force of a granular gripper. Granular Matter 23:1–6
30. Aktaş B, Narang YS, Vasios N et al (2021) A modeling framework for jamming structures. Adv Funct Mater 31(16):2007554
31. Athanassiadis AG, Miskin MZ, Kaplan P et al (2014) Particle shape effects on the stress response of granular packings. Soft Matter 10(1):48–59
32. Putzu F, Konstantinova J, Althoefer K (2019) Soft particles for granular jamming. Towards Autonomous Robotic Systems: 20th Annual Conference Proceedings, Part II
33. Löchte C, Kunz H, Schnurr R et al (2014) Form-flexible handling and joining technology (FormHand) for the forming and assembly of limp materials. Procedia CIRP 23:206–11
34. Jiang A, Ranzani T, Gerboni G et al. (2014) Robotic Granular Jamming: Does the Membrane Matter. Soft Robot 1
35. Howard D, O'Connor J, Letchford J et al. (2022) Getting a Grip: in Materio Evolution of Membrane Morphology for Soft Robotic Jamming Grippers. In: 2022 IEEE 5th International Conference on Soft Robotics (RoboSoft), pp 531–538
36. Howard GD, Brett J, O'Connor J et al (2022) One-shot 3D-printed multimaterial soft robotic jamming grippers. Soft Robot 9:1
37. FORMHAND Automation GmbH FH-R150. formhand.de/de/produkte/produkt-FH-R150. Acc. 01 Dec 2021
38. Kaufman RL (2013) Heteroskedasticity in regression: Detection and correction. Sage Publications
39. Cao B, Adutwum LA, Oliynyk AO et al (2018) How to optimize materials and devices via design of experiments and machine learning: demonstration using organic photovoltaics. ACS Nano 12:1
40. Elbadawi M, McCoubrey LE, Gavins FKH et al (2021) Harnessing artificial intelligence for the next generation of 3D printed medicines. Adv Drug Deliv Rev 175:113805
41. Akiyoshi M, Ikemoto K, Isobe H (2023) Tier-grown expansion of design-of-experiments parameter spaces for synthesis of a nanometer-scale macrocycle. Chemistry 18:2

Publisher's Note